Technical University of Denmark

DTU

Diode laser based light sources for biomedical applications

Müller, André; Marschall, Sebastian; Jensen, Ole Bjarlin; Fricke, Jörg; Wenzel, Hans; Sumpf, Bernd; Andersen, Peter E.

DTU Library
Technical Information Center of Denmark

Abstract Diode lasers are by far the most efficient lasers currently available. With the ever-continuing improvement in diode laser technology, this type of laser has become increasingly attractive for a wide range of biomedical applications. Compared to the characteristics of competing laser systems, diode lasers simultaneously offer tunability, high-power emission and compact size at fairly low cost. Therefore, diode lasers are increasingly preferred in important applications, such as photocoagulation, optical coherence tomography, diffuse optical imaging, fluorescence lifetime imaging, and terahertz imaging. This review provides an overview of the latest development of diode laser technology and systems and their use within selected biomedical applications.

670 nm external cavity diode laser for Raman spectroscopy built on a 13×4 mm^2 microbench (Copyright FBH/Schurian.com).

REVIEW ARTICLE
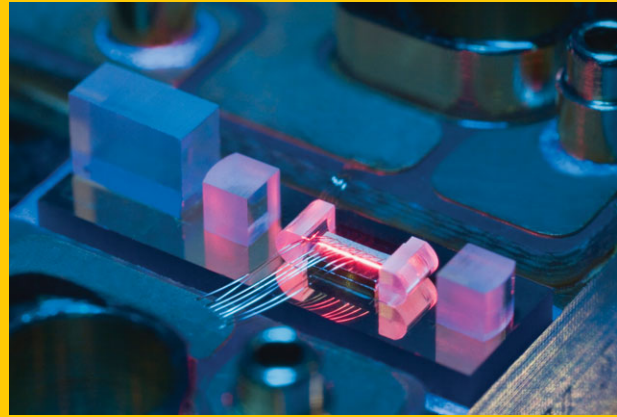
Diode laser based light sources for biomedical applications

André Müller[1,*], Sebastian Marschall[1], Ole Bjarlin Jensen[1], Jörg Fricke[2], Hans Wenzel[2], Bernd Sumpf[2], and Peter E. Andersen[1]

1. Introduction

Since the first practical demonstration of a laser by Theodore Maiman in 1960 [1], the range of applications has heavily increased. With improvements in production as well as performance, diode lasers also became increasingly attractive. Due to direct electrical pumping, diode lasers are by far the most efficient light sources currently available [2, 3]. Being based on chip technology, they can be manufactured in high numbers and at low cost. Their dimensions of only a few mm^3 enable very compact laser systems. All these features increase their application potential, including biomedical applications. Applications range from imaging and diagnostics, e.g., optical coherence tomography [4], fluorescence lifetime imaging [5], diffuse optical imaging [6], THz imaging [7], laser Doppler imaging [8] or Raman spectroscopy, to direct treatment such as photocoagulation [10], photo-dynamic therapy [11] or biomodulation and bioactivation [12].

Compared to lasers limited to specific atomic transitions, diode lasers cover a much wider spectral range. Depending on the used compound semiconductors and their composition, the emission wavelengths of typical III-V compound semiconductors range from blue to near-infrared (400 nm – 2 μm, [13]). Although spectral side modes are sufficiently suppressed at higher currents [14], the application of diode lasers may be limited by their spectral characteristics. In these cases, the emission bandwidth can be narrowed, e.g., by intrinsic [15] or external feedback [16]. The latter also enables single-mode emission tunable over several tens of nanometers [17], in addition to the tunability obtained by adjusting the injection current or the laser temperature.

Despite the number of wavelengths that can be accessed with diode lasers, the output power might not be sufficient. In addition, other wavelengths, especially in the visible range, may not be achievable due to lack of available laser structures. One option also to achieve these wavelengths, or to increase the output power at a certain spectral region, is nonlinear frequency conversion [18], as discussed in this article. Other options are optically pumped semiconductor lasers [19] or solid-state lasers [20], although not covered in the present review. Due to the optical excitation these lasers show reduced optical efficiencies compared to electrically pumped diode lasers [21].

The output power and the beam propagation parameters (M^2) of the diode lasers strongly depend on the design of the semiconductor structures. Nearly diffraction-limited beams are obtained with ridge-waveguide (RW) and tapered diode lasers. While the output power of RW lasers is limited to 1–2 W [22], more than 10 W are achieved with tapered lasers [23]. High-power emission is also obtained with broad area (BA) diode lasers [24] or diode laser bars and stacks [25]. However, these devices typically show reduced beam qualities that may be improved by additional feedback [26].

[1] DTU Fotonik, Department of Photonics Engineering, Technical University of Denmark, Frederiksborgvej 399, 4000 Roskilde, Denmark
[2] Ferdinand-Braun-Institut, Leibniz-Institut für Höchstfrequenztechnik, Gustav-Kirchhoff-Straße 4, 12489 Berlin, Germany
*Corresponding author(s): e-mail: amul@fotonik.dtu.dk
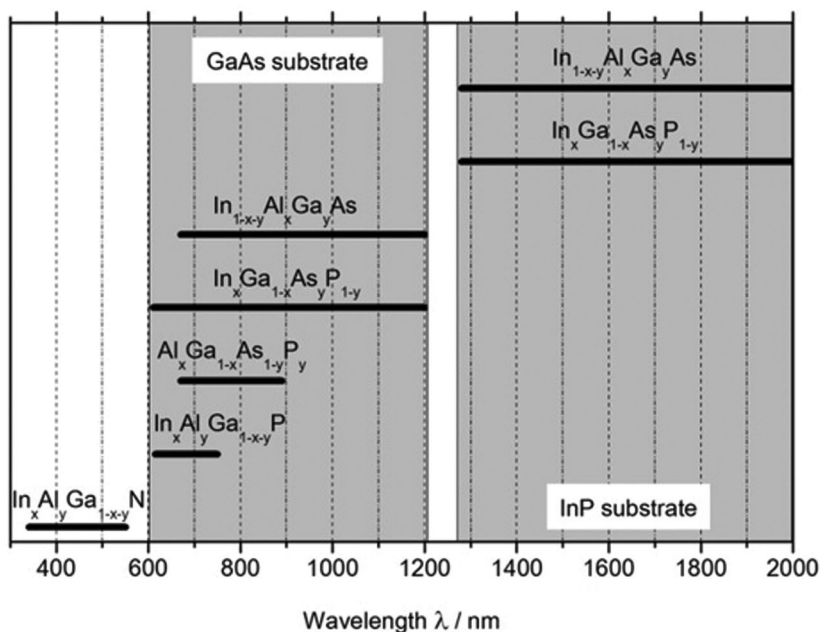
Figure 1 Compound semiconductor materials for the spectral range between 300 nm and 2000 nm.

All these devices are edge emitting diode lasers, i.e., the propagation of the generated laser emission is in plane with the substrate surface [27]. In surface emitting diode lasers, also known as vertical cavity surface emitting lasers (VCSEL), the propagation direction is normal to the substrate surface. Their optical cavities are short and the facet reflectivities are high, resulting in low threshold currents [27]. The output power is typically in the milliwatt range but can be increased significantly by optical pumping in so-called vertical external cavity surface emitting lasers (VECSEL) [28]. In comparison to edge-emitting diode lasers described in this article, the challenging factor towards high-power, near diffraction-limited emission from VCSELs is the proper heat removal from the active region [29].

In addition to continuous wave (CW) emission, diode lasers may also be operated in pulsed mode. Pulsed emission is achieved by mode-locking [34], Q-switching [31] or in a more direct manner by gain-switching [32]. These techniques enable the generation of pico- to femtosecond pulses with repetition rates in the GHz range. Compared to other mode-locked or Q-switched lasers, the lower upper-state lifetime of nanoseconds [33] reduces the obtained pulse energies of diode lasers [34]. However, generated pulses with up to 50 W peak power [35] are more than sufficient for applications such as fluorescence measurements, which will be discussed in the present review.

The above-mentioned characteristics, i.e., output power, beam properties, wavelength spectral coverage and tunability, compactness and low cost, make diode laser technology versatile and increasingly applicable in the biomedical field, in particular. In this review, we provide an overview of state-of-the-art edge emitting diode lasers and their use within key biomedical applications. At the end we give an out-look on the future perspective of diode lasers for emerging applications within the biomedical field.

2. Edge-emitting diode lasers

Two key advantages of diode lasers are their capability of covering a wide spectral range and the possibility of realizing different layouts with individual features. In this section we introduce the required material structures and explain how diode lasers are built up. At the end we focus on the performance of diode lasers with respect to the applications discussed in the article.

2.1. Material structures and fabrication of diode lasers

Several compound semiconductors have to be applied in order to cover the above mentioned spectral range between 400 nm and 2 μm. A coarse selection of the laser wavelength λ can be performed by adjusting the composition of the material, later given as molfraction x, y, z. An overview on the available group III-V-compound materials is shown in Fig. 1. In the blue to green spectral range $In_xAl_yGa_{1-x-y}N$ material is used [36, 37]. Red emitting diodes between 615 nm and 750 nm are based on $In_xAl_yGa_{1-x-y}P$. Between 670 nm and 890 nm $Al_xGa_{1-x}As_{1-y}P_y$ is used as an active layer. Longer wavelengths up to 1.2 μm can be reached using $In_xGa_{1-x}As_yP_{1-y}$ or $In_{1-x-y}Al_xGa_yAs$, grown on GaAs [38, 39]. Grown on InP substrates, the latter materials can cover the range up to 2.3 μm. Even longer wavelengths can be addressed by using antimonide based layer structures, lead salt lasers or more recently quantum cascade lasers.
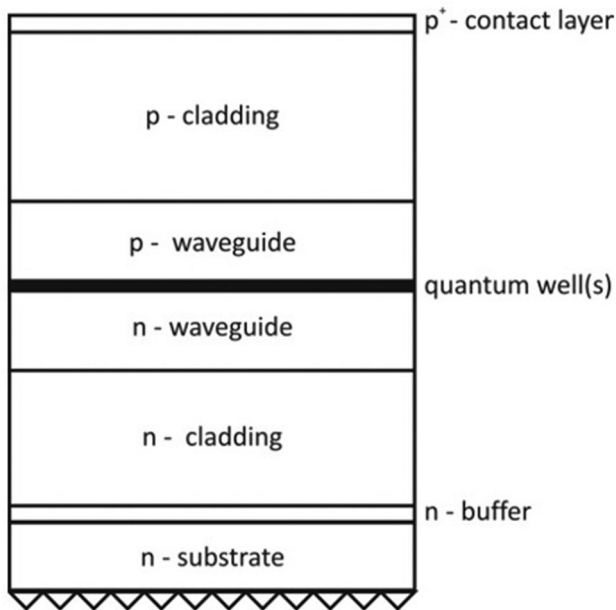
Figure 2 Scheme of a typical vertical layer structure of diode lasers.

The basic design of typical vertical layer structures is given in Fig. 2. The active layer consists of one or more quantum wells or quantum dots. This layer is embedded into a p- and n-side waveguide, which is surrounded by cladding layers. The p-side is completed by a highly doped contact layer. The layer structures are typically grown by metal organic vapour phase epitaxy (MOVPE) [40–44] or

molecular beam epitaxy (MBE) [45, 46] on different substrates with a diameter between 2–4 inch.

The wafers are processed into laser devices applying different lithographic, etching and plating technologies. Typically, a first lithography defines the stripe width along which the light is guided through the device. Two mechanisms can contribute to this guiding, index-guiding and gain-guiding. In order to achieve index-guiding, a ridge can be etched into the p-side waveguide layer as shown in Fig. 3a. The deep etching causes a step in the refractive index leading to lateral confinement. Typical RW lasers provide nearly diffraction-limited beam quality at output powers in the lower watt-range. For gain-guiding, typical for BA lasers, a conductive stripe is defined in the contact layer (Fig. 3b). This is done by destroying the conductivity outside the stripe using ion implantation or by etching a low MESA structure. Hereby the carrier injection and laser emission are limited to this area. The stripe width can be in the range from some 10 μm up to 800 μm. Such BA lasers reach significantly higher output powers up to some 10 W, but suffer from poor beam qualities with M^2 values typically in the range 10–50. To reach even higher output power several emitters can be combined within one laser bar (Fig. 3c), which reaches CW output powers of several 100 W.

In order to obtain high output power emission with good beam quality, one of the most promising concepts is the tapered laser. Within one chip, the diffraction-limited radiation of a RW section is coupled into a flared section (Fig. 3d), which can be realized index-guided or typically gain-guided. This section acts ideally as a passive amplifier [47–52]. In the flared section the mode-area is
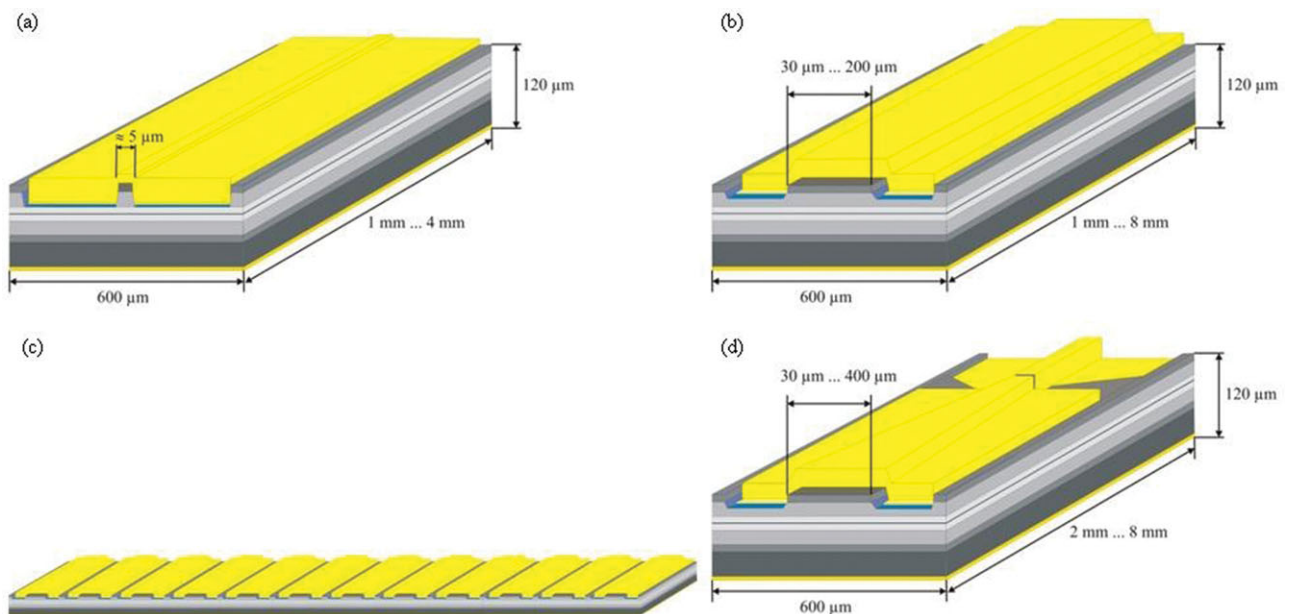
Figure 3 (online color at: www.lpr-journal.org) Illustrations of different diode lasers showing a ridge-waveguide laser (a), a broad area laser (b), a 12 emitter laser bar (c) and a tapered laser or amplifier (d).
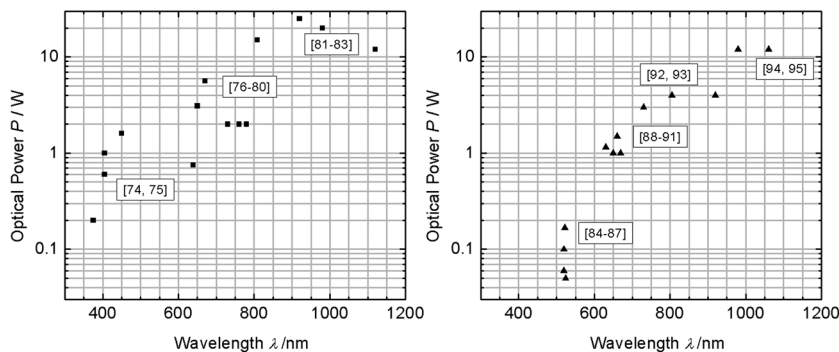
Figure 4 CW-output power versus emission wavelength for BA (left) and RW / tapered devices (right), including the reference numbers. In both cases the access towards high-power emission in the orange to violet range is limited. Higher output powers are achieved in the near-infrared with a maximum in the 9xx nm range. Typical for tapered devices shown here is that about 70% of the available output power is diffraction-limited.

slowly broadened while the single-transverse-mode profile is mostly maintained.

The emission linewidth of a diode laser can be stabilized and narrowed by introducing an internal grating into the resonator [53]. In the case of distributed feedback lasers (DFB), the grating spans over the entire resonator length [54–56, 57–59]. Alternatively, it is possible to implement the grating as distributed Bragg reflector (DBR), acting as a wavelength-selective resonator mirror [60–63].

Having defined and fabricated these structures, an appropriate metallization of the p-side of the device is performed, followed by a thinning of the substrate and the rear side metallization.

The processed wafer is cleaved according to the desired resonator length and facet coated. In order to achieve high output power, special care has to be given to the cleaning and passivation of the laser facets [64–66]. This process step is followed by an optical coating of the facets. For laser devices, the rear facet is coated with a high reflectivity $R_r \approx 96\%$, whereas the front facet is anti-reflection coated with $R_f \leq 30\%$. Using the devices as a gain medium in external cavity configurations, one side of the device is anti-reflection coated with an extremely low reflectivity $R_f < 5 \times 10^{-4}$. For devices used as amplifiers both sides have this low reflectivity.

In order to operate the devices, they are mounted on special heat sinks, providing an efficient heat removal. The most common approach is to mount the diodes p-side down, reducing the thermal resistance [67]. Long lasers with low thermal resistance can also be mounted p-side up, lowering the mounting induced stress [23]. First the laser is soldered on a submount. Depending on the laser devices different materials can be used. If the devices are mounted without any significant strain between the semiconductor and the mount, a submount material with a comparable thermal expansion coefficient might be selected, such as CuW, BN [68] or BeO [69, 70]. If heat removal is crucial and the devices are tolerant against strain, submount materials such as chemical vapor deposition (CVD) diamond [71] can be used. Alternatively, AlN can be applied; a relatively cheap material and easy to handle. As solder AuSn is often used, which guarantees a reproducible soldering process. Finally the diode laser submount is mounted on a copper block of different geometries. These copper blocks can be cooled passively (i.e. conductively) or actively using

micro-channel coolers. The fabricated laser diodes exhibit very long lifetimes up to several 10,000 h. Examples of such tests and the analysis of failures are reported in [72, 73].

2.2. Performance characteristics of diode lasers

All biomedical laser applications require certain parameters to be fulfilled. These can be, for example, wavelength, output power, beam quality, size and cost-efficiency of the laser systems. Diode lasers have proven their superior performance in these aspects. An overview on achieved maximum CW output powers at wavelengths between the blue and near-infrared spectral region is given in Fig. 4.

It is evident from Fig. 4 that diode lasers cover a large spectral range with increasing output power towards the near-infrared. Up to 25 W were obtained with broad area devices between 800–1000 nm [81]. This wavelength range coincides with a local maximum in the absorption spectra of blood. Even though the beam quality is rather poor, these lasers are extensively used in dermatology, because output power and wavelength rather than beam quality are the key parameters, as explained in Section 3.

In the red spectral range up to 5.6 W were reported for BA lasers [78]. Around 1 W was achieved with tapered devices [91]. The red to near-infrared wavelength region is preferred for diffuse spectroscopy and imaging, discussed in Section 7. Due to their size, efficiency, and power requirements in the order of milliwatts, diode lasers are preferably applied in these applications.

As Fig. 4 shows, obtaining high-power laser emission at shorter wavelengths in the visible range is still challenging. In the green spectral range up to 170 mW were demonstrated using ridge waveguide lasers [87]. With high-power green light being of high importance, for example, in dermatology and direct pumping of ultrashort pulsed lasers, frequency conversion represents a solution to increase the power at these wavelengths, as described in Chapter 5. Up to 12 W with near diffraction-limited beams were reported with tapered lasers at 978 nm [94] and 1060 nm [95]. Both types of devices were based on intrinsic DBR gratings as rear-end mirrors. Due to the high reflectivity of the intrinsic gratings, the rear facets of the lasers require antireflection coating. Therefore, spurious spectral modes are not reflected back into the tapered section and the

spectral linewidth is significantly narrowed [23]. Due to their output power and their excellent spatial and spectral characteristics these devices are ideal for frequency conversion into the blue-green spectral range. Combined with the large number of material compositions, frequency conversion of diode lasers also enables access to new wavelengths, currently not covered.

In the blue spectral range up to 1.6 W were shown with direct-emitting BA devices [74]. These wavelengths are preferably applied, for example, in fluorescence measurements typically requiring low power emission. One major challenge is to obtain yellow emission. This is mainly due to missing material structures for edge-emitting diode lasers around 590 nm or 1180 nm.

For any given structure or wavelength, pulsed emission is obtained simply by modulating the diode injection current. This enables generating pulses with adjustable pulsewidths and repetition rates suitable for applications, such as fluorescence based imaging. As explained in Section 6, the obtained peak power may be reduced compared to other laser systems, but still sufficient with respect to the sensitivity of biological targets.

It is obvious that based on their performance diode lasers become increasingly applicable in the biomedical field, and the following sections emphasize their advantages within key biomedical applications.

3. Direct application of high-power diode lasers in dermatology

As pointed out earlier, diode lasers provide increased output power in the near-infrared range. In dermatology these wavelengths combined with the absorption by blood are used to treat different diseases, such as vascular malformations and hemangiomas. Due to reduced absorption and scattering coefficients in tissue, corresponding diode lasers allow for longer penetration depths and the treatment of deeper-lying vessels. In addition, diode lasers address the need for compact and efficient systems. Their flexibility in wavelengths and the direct control of laser emission enable optimizing treatment parameters with respect to specific chromophores, the treatment outcome and reduction of side-effects.

3.1. Short introduction of selective photothermolysis

The application of lasers in the biomedical field is strongly related to light-tissue interactions. Such interactions enable both imaging as well as direct treatments. Light-tissue interactions can mainly be described and quantified by four different parameters: the refractive index, the scattering coefficient, the scattering phase function, and the absorption coefficient [96], respectively. While the scattering coefficient defines the probability of photon scattering events, the absorption coefficient provides information about the amount of energy being extracted from an incident light
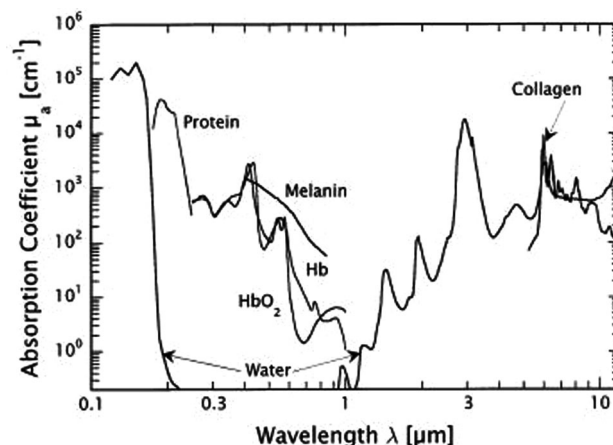
Figure 5 The plot shows the absorption coefficients of the main tissue components water, blood (oxy-hemoglobin HbO$_2$, deoxy-hemoglobin Hb), melanin, protein and collagen in the range of 0.1–10 μm (Printed with permission from [99]. Copyright (2003) American Chemical Society). Despite lower absorption, high-power diode lasers around 900 nm have the potential to make use of the 3rd oxy-hemoglobin absorption peak, for example, for photocoagulation.

wave. Their wavelength dependence [97] and the ratio between the scattering coefficient and the sum of the scattering and absorption coefficients, called the albedo [98], determine the penetration depth and therefore the optimum wavelengths for different applications.

In the visible range (400–600 nm) the absorption is dominated by oxy- and deoxy-hemoglobin, and melanin (Fig. 5). Above 1300 nm water is the main absorber. Within that window ($\approx$ 600–1300 nm) the absorption coefficients are reduced by 1–4 orders of magnitude.

The tissue response depends on the heat generated by absorption. Anderson and Parrish introduced selective photothermolysis, suggesting that selective tissue absorption within the so-called thermal relaxation time of the tissue leads to selective destruction of the target [100]. The thermal relaxation time is the time in which the targeted tissue dissipates 50% of the generated heat and it scales with the square of the target diameter. It therefore depends on the absorption coefficient and size of the target, as well as on the laser wavelength and pulse duration. The optimum pulse duration should be equal to or slightly less than the thermal relaxation time, in order to avoid damaging the surrounding tissue. For each target there is a critical temperature. Temperatures exceeding that value will lead to coagulation, vaporization, and finally ablation of the tissue, respectively [101].

3.2. Diode lasers for photocoagulation

In dermatology, selective photothermolysis is chosen for applications, such as hair removal [102], skin rejuvenation [103], or photocoagulation [104], respectively. The latter is

based on absorption of photon energy by blood and shall be the main application discussed in this section. Considering Fig. 5 the most obvious wavelengths for photocoagulation are in the green-yellow spectral range. Possible choices of lasers are, e.g., frequency doubled solid-state lasers, providing > 100 W of output power in CW or pulsed mode [105, 106]. These lasers tend to be bulky and expensive and thus alternative solutions are required. In addition, the very high absorption of blood in the green-yellow spectral range limits the penetration depth and the size of the vessels treated. Lasers with lower absorption are preferred to enhance volume heating of deeper-lying, larger vessels. In addition, a lower absorption in melanin has the potential to cause less damage to the skin. The main attenuation stems from the light scattering, which is reduced inversely proportional with wavelength. Hence, increasing the wavelength enhances penetration depth.

Accordingly, in Fig. 5 a trade-off solution to this problem is shown. The hemoglobin absorption curves also exhibit a local maximum in the range between 800–1000 nm and, simultaneously, the absorption in melanin is reduced. At these wavelengths, light experiences less scattering [97], increasing the penetration. However, the absorption coefficient of hemoglobin is reduced by more than one order of magnitude but still sufficient to obtain the effect. Available diode lasers are capable of emitting multiple tens of watts [81, 82] and can easily be coupled into multimode fibers for direct delivery. By providing sufficient optical energy in the most efficient and compact manner, whilst the beam propagation parameters not being crucial, these high-power, near-infrared diode lasers have become very attractive light sources for photocoagulation.

3.3. Treatment of vascular malformations and hemangiomas with diode lasers

3.3.1. Endovenous laser treatment of vascular malformations

Vascular malformations are disorders of blood or lymphatic vessels causing reddish or bluish lesions underneath the skin [104]. For example, venous malformations are common disorders where the valves within the veins are unable to prevent the reflux of blood causing swelling, pain and muscle cramps. The surgical treatment of choice is ligation and stripping of the veins leading to complications such as trauma, bleeding and scars, as well as increased hospital costs and long recovery times [107]. The non-surgical procedure is sclerotherapy, which can also cause pigment changes and scarring [108].

An alternative method is endovenous laser treatment (EVLT), a minimally invasive method introduced for the treatment for varicose veins [109]. The heat generated by absorption diffuses through the blood and vessel walls initiating the development of steam bubbles that cause thermal injury and vessel occlusion [110].

The light energy of a high-power, long-pulsed, fiber-coupled laser is delivered directly into the vein through the fiber and guided by ultrasound imaging. The light pulses are initiated while the fiber is slowly withdrawn causing vessel closure. Compared to sclerotherapy, EVLT enables a more precise control of vein wall damage, lowering the recanalization rates of the closed vessels.

Diode lasers are the lasers of choice for EVLT. They provide the necessary power level and wavelengths in fiber-coupled packages enabling compact and cost-efficient laser systems for the treatment. Furthermore, the amount of energy can be precisely controlled directly by the laser current. The first demonstration of a diode laser EVLT was carried out using a 14 W, 810 nm laser [109]. The actual procedure was carried out with 3–4 W delivered in 1–2 second pulses, required due to the blood flow dissipating the heat. The treated veins had mean diameters of 5 mm and lengths of 20 cm. The immediate results indicated an excellent closure rate of 100% comparing favorably to other minimally invasive techniques. These results were confirmed by other groups [107, 110–113]. A study of the short-term efficacy of EVLT showed that 99% out of 90 cases still showed vessel closures after 9 months follow-up [107]. The patients were instructed to walk immediately after the procedure and continue their normal daily activities, indicating the viability of the procedure. The risk factors for nonocclusion are not only related to laser parameters, such as fluence (energy per cm^2) or irradiation time, but also to physiological parameters such as the vein diameter and the distance of the thrombus to a larger vessel after the procedure [114]. Therefore, accurate diagnosis is of paramount importance in determining the proper laser and its parameters, in order to optimize the outcome of these treatments and minimize side-effects.

3.3.2. Treatments of vascular malformations applied externally

While EVLT requires the light to be delivered through a fiber via minimally invasive surgery, other procedures, such as the treatment of port-wine stains or telangiectasia [115], rely on the energy being delivered directly through the skin. The success of these treatments relies on the combination of light absorption and penetration depth. For small vessel sizes, green-yellow lasers like solid state lasers or dye lasers are chosen [116]. For larger vessels, deeper penetration is required. As discussed above, deeper penetration is achieved at longer wavelengths, obtained, for example, with near-infrared diode lasers. However, diode lasers are typically not preferred for treatments of these mostly superficial malformations. Nevertheless, a few groups did examine their capability in that field [117–121].

In one example, vascular abnormalities were treated with 150 ms pulses of a 980 nm laser at 300–500 J/cm^2 [120]. As mentioned above, longer wavelengths and short pulses increase the potential causing less damage to the skin. In another study laser therapy was combined with radiofrequency. In that case, the absorption of 250 ms laser

pulses preheated the blood vessel and created conditions for selective radiofrequency applications [121]. As a consequence, this combination allowed reducing the laser fluence (80–100 J/cm^2), lowering the risk of possible damages to the epidermal layer even further. The overall response of the patients in that study was excellent showing 75–100% lesion clearance.

3.3.3. Treatment of hemangioma by diode laser surgery

In comparison to vascular malformations, hemangiomas are vascular tumors developing after birth and regressing after a couple of years [104]. However, in case of symptoms such as bleeding, pain or functional compromise, treatment is strongly recommended. One preferred treatment is endolesional diode laser surgery [122]. As mentioned above, diode lasers provide sufficient output power in fiber-coupled packages, enable compact and cost-efficient laser systems, and the amount of energy at the desired wavelength can be controlled by the laser injection current.

Using a 980 nm diode laser delivering 3–12 watts in continuous or long-pulsed mode, 160 pediatric patients were treated with head and neck hemangioma up to 7 cm in size. The results showed that diode laser treatment improves individual results for lesions up to 5 cm. A similar laser was used performing soft tissue surgery of oral hemangioma [123]. The diode laser was chosen due to its ability to cut with high ablation capacity and reduced bleeding rates, while simultaneously coagulating soft tissue [124, 125]. It was noted that the removed specimens can have a size ≤ 5 mm to still enable a reliable histopathological diagnosis [126]. The diode laser emission led to a sufficient hemostasis and precise incision margins without the need for suturing after surgery [127]. Compared to competing lasers the same group concluded that diode lasers enabled

cutting comparable to CO_2 lasers and coagulation similar to Nd:YAG lasers [127]. All these results confirm that diode lasers are competitive choices in soft tissue surgery.

Based on their advantages high-power diode lasers are increasingly preferred within applications in dermatology. The range of wavelengths that are accessed with diode lasers open a range of new opportunities, compared to competing systems. Combined, these wavelengths, the resulting penetration depths and the obtained output powers enable addressing individual treatment parameters in a highly efficient manner, while satisfying the need for compact, portable and low-cost laser systems. These advantages combined with the continuous work in diode laser technology will increase the number of direct diode laser applications in the biomedical field even further.

4. Wavelength-swept diode laser systems for optical coherence tomography

Optical coherence tomography (OCT) is an interferometric technique that generates cross-sectional images of scattering material with a typical depth resolution of a few micrometers [128]. Rapidly wavelength-swept laser light sources, or simply *swept sources*, make ultra-fast OCT image acquisition possible. Semiconductor diodes are ideal gain media for these swept sources, as they permit broadband wavelength tuning at very high speed.

4.1. Optical coherence tomography

Due to the unique ability to image the morphology of biologic tissues non-invasively (Fig. 6, left), OCT has become a well-established tool for biomedical research and clinical diagnostics [129]. It is used on regular basis for early
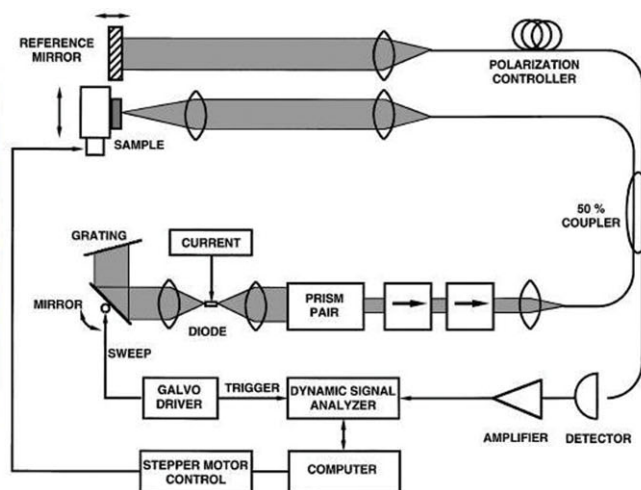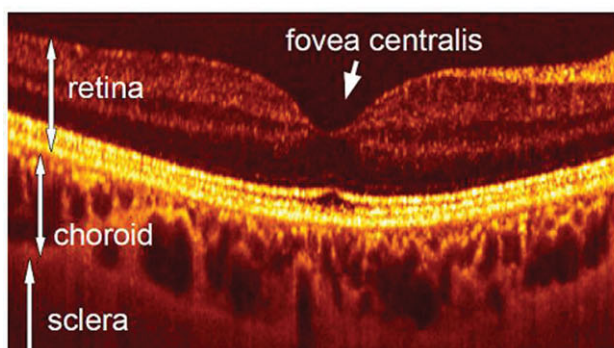
Figure 6 (online color at: www.lpr-journal.org) Based on interferometry, OCT creates high-resolution cross-sectional images of light-scattering samples, for instance of the human retina in vivo (left, courtesy of C. Hitzenberger, Med. Univ. Vienna). Like in this early swept source OCT system (right, printed with permission from [133]), the typical light sources are external cavity lasers featuring a semiconductor gain element in conjunction with a tunable bandpass filter.

detection of retinal pathologies and for monitoring treatment of those. Another clinical application is examining atherosclerotic plaques and coronary stents in cardiac blood vessels with endoscopic OCT systems. OCT is being used in many other fields of medical and biologic research, but also for technical purposes, such as non-destructive material testing or contact-free metrology [130].

An OCT system probes the sample with a beam of light (typically near-infrared), and obtains a depth-resolved reflectivity profile from the backscattered fraction. One such measurement is called an A-scan in analogy to ultrasound imaging. By scanning the beam laterally over the sample, a two- or three-dimensional image can be assembled from a number of adjacent A-scans. Most state-of-the-art OCT systems acquire A-scans in the frequency domain, i.e. by detecting the spectrum of the backscattered light after interference with a reference beam. They employ either broadband illumination and a spectrometer or a tunable narrowband light source and a fast photodetector [131,132]. In the latter scheme (Fig. 6, right), the light source performs rapid sweeps over a broad wavelength range [133, 134], hence this method is termed swept-source OCT (SS-OCT). While SS-OCT requires more complex light sources than spectrometer-based OCT, it offers a number of advantages, such as longer imaging depth range [135], lower susceptibility to artifacts caused by sample motion [136], and the possibility of ultra-high speed image acquisition [137,138].

4.2. Special properties of swept sources

Most swept sources are tunable lasers in highly specialized configurations that meet the requirements for OCT. State-of-the-art swept sources feature sweep repetition rates ranging from 100 kHz up to several MHz. The tuning bandwidth can be well above 100 nm, which is desirable since the OCT depth resolution improves proportionally with the bandwidth [129]. On the other hand, the dynamic linewidth, i.e.

the instantaneous width of the narrowband spectrum while it is being tuned, is rather broad compared to classical CW laser lines. Up to several 10 GHz may be acceptable, which results in an OCT imaging depth range of a few millimeters [134, 139, 140]. In recent years, however, considerable efforts went into the development of swept sources with narrower dynamic linewidth in order to increase the imaging depth range [141–144].

The very high tuning speeds of 10^7–10^8 nm/s can only be realized using semiconductor laser gain media, which feature a short excited-state lifetime on the order of nanoseconds. Other swept source configurations based upon doped crystals or fibers did not show good performance at high sweep rates [134, 145, 146].

Semiconductor gain media have also a number of other advantages. They are available for many different wavelength ranges and offer broad gain bandwidths as well as unmatched flexibility for tailoring the gain spectrum. Due to direct electrical pumping, light sources can become very efficient and compact. It also permits straight-forward arbitrary shaping of the light source spectrum, which is useful for optimizing the OCT signal acquisition [147–149] and allows to correct for spectrally dependent transmittance of optical media in the probing beam path [150].

4.3. Swept source technology

Today, most swept sources in practical applications are external cavity tunable lasers (ECTLs) using a semiconductor optical amplifier (SOA) – i.e. a diode with single-mode waveguide and anti-reflection coated facets – as gain medium and a tunable band-pass filter in either a free-space or fiber-based setup. Free-space resonators can be very compact [151], especially in conjunction with a tunable filter based upon micro-electro-mechanical systems (MEMS) [152, 153].

Fiber-based setups (Fig. 7), on the other hand, which offer uncomplicated implementation of stable,
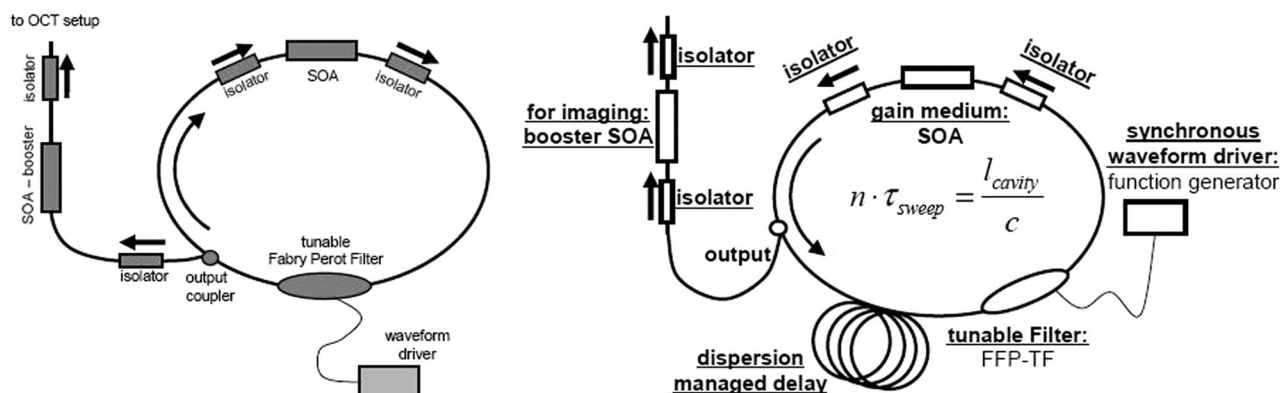
Figure 7 Fiber-coupled semiconductor optical amplifier modules and other fiber-optic components enable stable and alignment-free swept source setups. In contrast to a standard ring-laser (left, printed with permission from [154]), a Fourier domain mode-locked laser (right, printed with permission from [155]) features a very long resonator required for synchronizing the filter sweep period, τ_{sweep}, with the resonator round-trip time. l_{cavity}: optical length of the laser resonator, c: speed of light, n: integer number, SOA: semiconductor optical amplifier, FFP-TF: fiber Fabry-Perot tunable filter.

alignment-free light sources, are preferred by the research community [139, 140, 154]. Furthermore, by using a long fiber resonator (several 100 to 1000 meters) one can synchronize the sweep rate of the tunable filter with the resonator roundtrip frequency [155]. Using this technique, called Fourier domain mode-locking (FDML), one can overcome the tuning speed limitation given by the time required to build up laser light from spontaneous emission. Whereas ECTLs with short resonators have been demonstrated with sweep rates up to 400 kHz [156], more than 5 MHz could be achieved with an FDML laser [137].

Currently, two promising alternative technologies for high-speed swept sources are emerging. Both aim for compact diode lasers with integrated tuning mechanisms, which are suitable for cost-effective mass production. One approach is based on VCSELs with a MEMS-actuated top mirror that can change the resonator length. These devices operate inherently on a single optical frequency, tunable without mode-hops, and feature hence a narrow dynamic linewidth. Recently, OCT imaging with a VCSEL-based swept source was demonstrated, that supports broadband tuning with sweep rates up to 1 MHz and permits imaging over a depth range larger than 50 mm [157, 158]. The other approach is a monolithic diode laser tunable with DBRs in a Vernier-configuration [144]. While these devices require complex control electronics for a broadband sweep without mode-hop artifacts, they offer unprecedented flexibility for adjusting the light source characteristics to various purposes. This technology appears promising for versatile high-speed swept sources, enabling long imaging depth ranges.

4.4. Output power of semiconductor based swept sources

Semiconductor chips emitting a single-transverse-mode beam, which is essential for imaging applications, provide relatively low optical power in the range of a few tens of milliwatts. This is sufficient for many OCT systems, since the probing beam intensity on living tissue must not exceed the safety limits. However, depending on the specific application and the system architecture, there can be a demand for an increased output power. This can be achieved with an additional optical amplifier either as a booster at the output or as an extra gain element in the laser resonator. Different configurations have been demonstrated employing another standard SOA [154, 159], a tapered semiconductor amplifier [160], or a rare-earth-doped fiber amplifier [148, 161].

Although there are many different ways to implement a swept source for OCT, high performance depends in all cases critically on the unique features of semiconductor laser gain media. Hence, the advantages of swept-source OCT, such as ultra-high-speed image acquisition and long imaging depth range, could not have been developed that far without semiconductor laser technology.
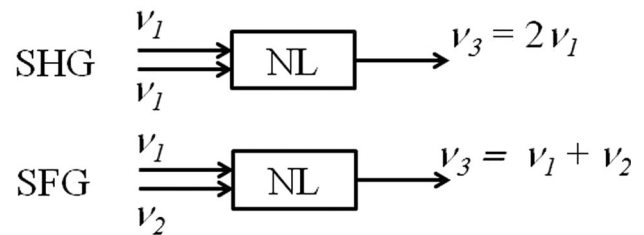
Figure 8 In the cases of SHG and SFG two photons, incident on a nonlinear crystal (NL), are converted into a single photon with the same energy as the sum of the two input photons. The parameter υ represents the corresponding frequency of incident and generated photons.

## 5. Extending the spectral range by nonlinear frequency conversion

As demonstrated in Section 2, the emission wavelengths of diode lasers range from the blue to the near-infrared spectral range. However, the output power at certain wavelengths can still be limited. Nonlinear frequency conversion represents a means to overcome these limitations. In conjunction with the number of available emission wavelengths from diode lasers, this technique also enables the design of compact and efficient modules covering new wavelengths. Obtaining optimum performance requires high-power emission with good spatial and spectral characteristics, as provided by, for example, tapered diode lasers.

5.1. Short introduction of nonlinear frequency conversion

Figure 8 illustrates the basic principle of nonlinear frequency conversion for the cases of second harmonic generation (SHG) and sum-frequency generation (SFG). Using a bulk nonlinear crystal, the power of new photons generated from incident photons scales with the square of the fundamental pump power and the nonlinear coefficient. In addition, it scales linearly with the length of the crystal [162], as well as with the "Boyd-Kleinman factor", determining the optimum focus spot size with respect to the crystal length [163].

The most important aspect for efficient frequency conversion is to obtain phase matching, i.e., waves involved in frequency conversion propagate at the same phase velocity [165]. This is in general achieved by optimizing the crystal temperature, the crystal position or the fundamental wavelengths. The phase matching acceptance bandwidths decrease linearly with increasing crystal lengths, thus becoming narrower for longer crystals [166].

In summary, in order to obtain optimum results, the lasers should provide high power emission with nearly diffraction-limited beam qualities [164] and narrow spectral widths. The nonlinear crystals should be chosen accordingly.
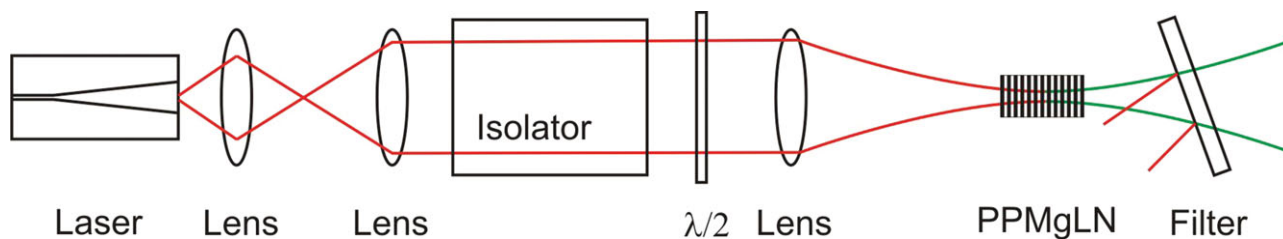
Figure 9 (online color at: www.lpr-journal.org) The basic setup for single-pass frequency conversion consists of a collimated laser, a focusing lens and a temperature controlled nonlinear crystal. In this example a tapered diode laser is frequency doubled using a periodically poled magnesium-doped lithium niobate crystal (PPMgLN). Using diode lasers additional optical isolation may be required to avoid optical feedback to the diodes. In that case a half-wave plate is used to readjust the polarization as required by the nonlinear crystal. A filter or dichroic mirror is used to separate the fundamental and generated beams. Single-pass frequency conversion can be realized with bulk crystals as depicted here, or with nonlinear waveguide crystals. The confinement in nonlinear waveguides increases the conversion efficiency but the performance can be limited by thermal non-uniformities at high pump powers [168].

5.2. Concepts for nonlinear frequency conversion

The most straight-forward approach for frequency conversion is a single-pass configuration (Fig. 9). Light at the fundamental wavelength is directly focused into the nonlinear crystal. Behind the crystal the fundamental and generated waves can be separated by a filter or dichroic mirror. Using this scheme, conversion efficiencies with more than 50% have been reported with diode lasers [167].

Higher efficiencies are possible by allowing multiple passes through the crystal. This can be done by external cavity, intra-cavity, multiple-pass or cascaded frequency conversion [169–172]. In these cases the crystal is either positioned inside a resonator or multiple passes in one or consecutive crystals are used to increase the effective length of the nonlinear material. All concepts are increasingly complex but lead to higher conversion efficiencies [105,173–175].

5.3. Biomedical applications in the visible spectral range

One common application for blue-green lasers is direct pumping of titanium:sapphire (Ti:S) lasers [177]. These lasers generate femtosecond pulses based on very broad emission bandwidths (>100 nm) in mode-locked operation [178]. High-intensity, short pulses are required for many biomedical applications, e.g., two-photon microscopy [179] or coherent anti-Stokes Raman scattering microscopy [180].

Direct pumping is in most cases done by frequency doubled solid state lasers, having low electro-optical efficiencies and significantly adding to the dimensions and price of Ti:S laser systems. Switching to direct green light emitting diode lasers is still challenging. Indium gallium nitride (InGaN) based laser diodes emitting up to 170 mW (CW) were demonstrated but their performance is limited by the laser crystal qualities [84–87]. As an alternative, 1060 nm DBR-tapered diode lasers were presented [23]. These diode lasers fulfill all requirements for efficient frequency conversion: high-power laser emission, nearly diffraction-limited beams and narrow spectral bandwidth tunable by adjusting the laser temperature. Based on these lasers more than 1.5 W of green light were generated by single-pass SHG and a similar laser later demonstrated its potential in competitive direct pumping of Ti:S lasers [181, 182]. In an alternative approach, Jedrzejczyk et al. achieved 1 W at 532 nm using a nonlinear, planar crystal waveguide [183]. At 490 nm, a wavelength closer to the maximum absorption of Ti:S crystals, a compact version of a frequency doubled DBR-tapered diode laser was presented. This laser system generated 1 W of blue-green radiation on a footprint of only 50 × 10 × 5 mm^3 [184].

Using diode lasers, the power available for frequency conversion is limited by thermal degradation and beam filamentation at high currents [185]. Therefore, different approaches have to be used to push their performance even further. One recently demonstrated approach is sum-frequency generation of two beam-combined tapered diode lasers [186]. Using this scheme the power available from frequency converted diode lasers was increased to nearly 4 W of green light. At this level diode lasers have a strong application potential treating vascular lesions, currently carried out with 532 nm KTP lasers [187–189].

The UV-blue spectral range is suited for biomedical applications, such as soft tissue surgery, cytometry, cell transfection or fluorescence measurements [190–193]. A 318 mW, 404 nm frequency doubled diode laser was shown suitable for drug quantification measurements in a mouse model as part of photodynamic therapy [194, 195]. The fluorescence initiated by the diode laser radiation helped to examine the drug uptake as well as its distribution, giving information about the location of tumors and its boundaries to healthy tissue. By combining the advantages of diode lasers and solid state lasers, many wavelengths can be obtained by SFG. As an example, 300 mW at 488 nm was demonstrated [196]. By exchanging the diode and/or solid state laser, almost any wavelength can be efficiently generated using this method. Much higher output power was generated by intracavity frequency doubling of a 49 emitter laser bar, resulting in 1.2 W at 465 nm [197]. The

latter was realized in a compact scheme with only 4.4 cm in length, demonstrating again the possibility of very compact high-power laser systems.

One strong competitor to frequency doubled blue diode laser systems are direct-emitting gallium nitride (GaN) lasers. Most biomedical applications in this spectral region are low power procedures. With the development of GaN lasers these requirements can be matched in an even more efficient way than by frequency conversion. These lasers are capable of generating the required output power [198] and already have or are about to replace low power, frequency conversion based systems.

In the yellow spectral range, the absorption characteristics of the main tissue components are similar to green radiation, however with a reduced absorption coefficient for melanin. Corresponding lasers have the potential to reduce skin damage compared to green radiation during the treatment of, for example, vascular lesions. Unfortunately, these wavelengths are currently not covered by frequency converted diode lasers. This is mainly due to missing material structures for edge-emitting diode lasers around 1180 nm. Nevertheless, up to 5 W of yellow light were already demonstrated by intracavity frequency doubling of an optically pumped semiconductor laser [199]. This type of laser is also based on a semiconductor chip. However, as the name suggests, two conversion processes are needed to generate yellow light, reducing the overall efficiency.

After the first demonstration of frequency conversion in 1961 [200], its use in combination with diode lasers has become an established technique to gain access to new wavelengths. In addition, the advent and use of micro-optics further enable the realization of ultra compact and portable modules. Although low power applications will sooner or later be carried out mostly by direct emitting visible diode lasers, frequency conversion of diode lasers will be the method of choice when compact and efficient modules with increased output power at accessible or new wavelengths are required.

6. Gain-switched diode lasers generating optical pulses down to the picosecond range

Two key advantages of diode lasers are their large number of available wavelengths and the ability of controlling the emission by the injection current. Some applications within the biomedical field require light to be delivered in pulses. In this chapter we explain how gain-switched diode lasers are used to generate these desired pulses, precisely matching the requirements of the application in form of wavelength, pulsewidth and repetition rate. Due to their short carrier lifetime, the obtained pulse energy and peak power may be reduced compared to other lasers. However, in the biomedical field their performance is more than sufficient for, e.g., fluorescence based imaging techniques. In addition, external amplification can be used to boost the power if necessary.

6.1. Fluorescence based imaging techniques

Fluorescence based imaging, such as fluorescence tomography (FT) or fluorescence lifetime imaging microscopy (FLIM), relies on measuring the spatial distribution of the fluorescence intensity inside a sample (FT) or on measuring the decay rates of different lifetimes of fluorophores (FLIM) [201]. The information gained from these techniques can help to evaluate physiological aspects [202–204] or to locate fluorophores in cells or tumors [205–209]. The required light sources should typically provide picoseconds pulses with sufficient output power and variable repetition rates and pulse widths. The latter two are required to avoid photo-bleaching [210] and to detect different fluorophores properly.

6.2. Generating pulsed laser emission

Using lasers, pulses are generated in different ways [211]. One option is mode-locking, i.e., the coupling and phase-locking of multiple modes by periodically modulating the losses inside the laser resonator in an active or passive manner. The repetition rates of the generated pulse trains are fixed and correspond to the round-trip time of the resonator [212]. In comparison, Q-switching is an established technique where pulsed operation is achieved by periodically switching between high and low resonator losses, i.e., changing the "Q-factor" of the laser resonator. This technique is mostly applied in solid state laser systems. Constant optical pumping at high resonator losses causes the pump energy to be stored in form of population inversion, and released as a short pulse, once the losses are switched. This allows adjusting the pulse widths and repetition rates as required for the applications. Using diode lasers instead, the amount of stored energy and therefore the peak power is limited by the short carrier lifetime. A third option is cavity dumping [211], an active technique often in conjunction with either of the other two. All three methods rely on a cavity configuration, increasing the complexity and size of the optical system.

A much more direct approach towards pulsed emission with the desired features is gain-switching of diode lasers [211]. This technique is utilizing the generation of diode laser emission by direct electrical pumping. Pulses are generated simply by modulating the injection current to the diodes, allowing for variable pulse durations and repetition rates from the Hz to GHz range. Due to the simple scheme, gain-switched diode lasers can be realized much more compact and user-friendly. The high repetition rates are made possible by the short carrier lifetimes in diode lasers. As a trade-off, this short carrier lifetime also limits the energy storage and thus the maximum pulse energy and peak power.

6.3. Examples for gain-switched diode lasers

Gain-switched diode lasers were demonstrated in the visible [213] and near-infrared spectral range [214]. In both

cases pulse widths down to a few tens of picoseconds were generated. The latter also showed the possibility of diffraction-limited and wavelength stabilized pulsed emission using the characteristics of DFB or DBR diode lasers, as described in section 2.1. Using an additional saturable absorber within the diode laser chip even enables shaping the pulse spectrum [215, 216]. The obtained peak powers of gain-switched diode lasers can easily reach up to a few watts [214]. In order to achieve higher output power, additional amplification may be necessary. This can be realized by different methods using, e.g., fiber amplifiers, semiconductor optical amplifiers or tapered amplifiers in form of a master oscillator power amplifier (MOPA) configuration [217–222]. Using the latter scheme up to 6.5 kW of peak power were demonstrated [221].

In order to obtain other wavelengths frequency conversion has been applied to generate short pulse emission, e.g., in the green, yellow, and near-infrared spectral range [217, 218, 222, 223], respectively. The green spectral range can easily be obtained by frequency doubling ps-pulses at around 1060 nm. In contrast to this approach, the yellow spectral range was accessed by sum-frequency generation of a gain-switched diode laser at 1.5 μm and the residual pump light at 976 nm required for fiber amplification of the generated pulses (Fig. 11). For the near-infrared range around 750 nm a similar 1.5 μm gain-switched diode laser was frequency doubled. This laser was then applied for direct pumping of photonic crystal fibers, generating a supercontinuum (450–1200 nm, [223]).

As mentioned above, lasers applied in fluorescence measurements should ideally provide picosecond emission with sufficient output power, variable repetition rates and adjustable pulse widths. It becomes obvious that gain-switched diode lasers represent the most direct approach towards short picoseconds pulses and can fulfill the requirements in an efficient and compact manner. Therefore, they are well suited for such applications and different groups have already demonstrated gain-switched diode laser based FLIM or FT systems in the visible or near-infrared spectral

range [202, 208, 224–227]. The possibilities of subsequent amplification or frequency conversion enable higher peak powers and increase the number of available wavelengths, giving diode lasers a strong standing in the field of biomedical pulsed laser applications.

## 7. Diffuse near-infrared spectroscopy and imaging using diode lasers

As mentioned above, light tissue interactions are mainly characterized by scattering and absorption [96]. Light reemitted by the tissue contains information about absorption and scattering effects. These effects can be decoupled with proper algorithms to obtain information about the optical properties of the tissue [6, 228–231]. This is the basis for non-invasive, diffuse near-infrared (NIR) spectroscopy and imaging in soft tissue. While spectroscopy allows measuring time-dependent variations of the optical properties, e.g. oximetry measurements, imaging is used to locate heterogeneities in tissue, such as tumors or aneurysms [232]. In this chapter we show that diode lasers are preferred in this field, due to their capabilities of generating picoseconds pulses in the order of milliwatts at high repetition rates.

7.1. Near-infrared systems for diffuse spectroscopy and imaging

There are three different techniques to measure the optical properties [6, 233], which are carried out in a planar or a cylindrical configuration; CW, time-domain, and frequency-domain, respectively. For all of the techniques, the basic principle relies on at least one laser source illuminating the target. The reemitted light is in most cases measured by multiple detectors. In CW imaging [234, 235] the time invariant distribution of the light intensity is recorded at multiple positions. This technique is simple, requires only one source-detector pair but needs calibration to obtain
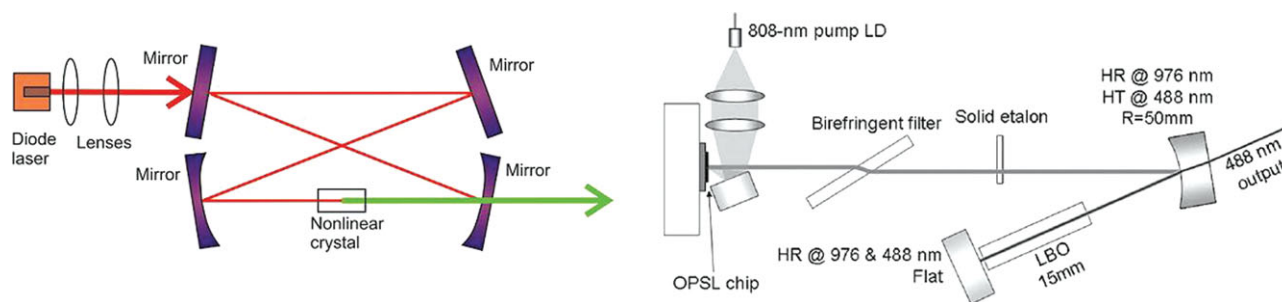
Figure 10 (online color at: www.lpr-journal.org) Two examples of external and intracavity frequency conversion. In both cases the nonlinear crystal is positioned inside a resonator. Compared to a typical single-pass configuration, curved mirrors are used to focus the fundamental wave inside the nonlinear crystal. For external frequency conversion the nonlinear crystal is often positioned inside a bow tie resonator (left). Inside the cavity the intensity of the fundamental wave increases, leading to higher conversion efficiencies. Additional components may be required to realize unidirectional cavities. The resonator for intra-cavity frequency conversion also contains the laser gain medium (right, printed with permission from [176]). In our example a semiconductor laser chip is optically pumped by an external laser diode and then frequency converted using a lithium triborate (LBO) crystal.
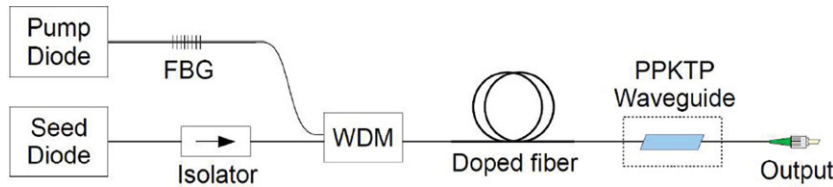
Figure 11 (online color at: www.lpr-journal.org) One approach towards picosecond pulses at new wavelengths is sum-frequency generation. In this example sum-frequency generation is carried out using a gain-switched, fiber Bragg grating (FBG) stabilized diode laser and the residual pump light required for fiber amplification (printed with permission from [218]). A periodically poled potassium titanyl phosphate crystal (PPKTP) is used for frequency conversion.

absolute values of the optical properties. Time-domain imaging is based on light sources providing short pulses [236–243]. The optical properties are obtained by measuring the time of flight distribution, the time it takes from source to detector. The signals are measured using either expensive streak cameras or time-consuming single-photon-counting systems (Fig. 12). Note that the time-domain imaging technique provides the highest information content of the three methods [6].

The most common approach is frequency-domain imaging [44–54]. In this case the laser light intensity is modulated (Fig. 12), for example, sinusoidal. The propagation in heterogenic biological tissue leads to perturbations of amplitude attenuations and phase shifts, from which the optical properties are calculated. In order to obtain good signal-to-noise ratio the product between the time delay experienced by the waves and the angular frequency should be close to unity [255]. In NIR spectroscopy and imaging the typical time delay for source-detector separations of a few centimeters is in the order of 1 ns. This consequently requires the laser to be modulated at around 100 MHz.

The most obvious laser sources for these measurements are diode lasers. They provide sufficient output power

(Fig. 4), which in this case is in the order of milliwatts in the red to near-infrared range, and their rapid response enables the emission of picoseconds pulses and an intensity modulation up to the GHz range [256].

The main components in biological soft tissue are water, blood (oxy- and deoxy-hemoglobin) and lipids. Due to their difference in absorption spectra, a sufficient number of wavelengths have to be used to increase the sensitivity and specificity of these techniques [254]. While dual wavelength spectroscopy is well established to determine the oxygen concentration in blood [257], systems with up to seven lasers have been demonstrated to study the composition and physiology of the tissue [254]. Using diode lasers, the required wavelengths (typ. 670 nm $< \lambda <$ 980 nm) are provided in a compact, cost-efficient manner.

7.2. Applications based on diffuse NIR spectroscopy and imaging

Major applications in NIR imaging and spectroscopy are cancer detection, e.g., in the breast or brain, or observing
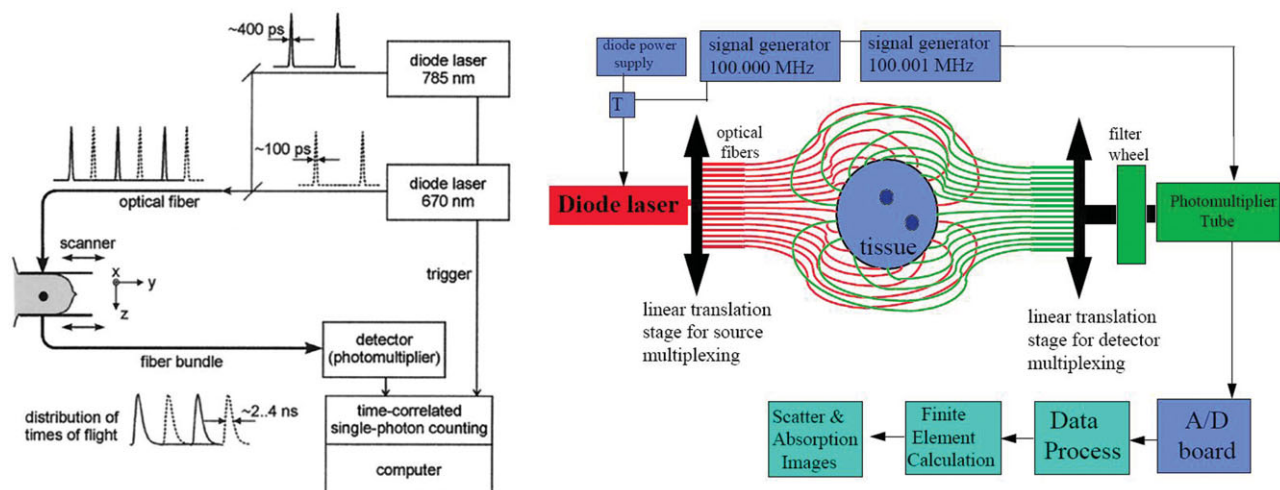
Figure 12 (online color at: www.lpr-journal.org) In a time-domain imager the target is illuminated by picosecond laser pulses (left, printed with permission from [243]). A streak camera or as shown here a single-photon counting system are used to measure the time of flight distribution resulting from absorption and scattering events. A frequency domain imager is based on a modulated laser source (right, printed with permission from [244]). During the propagation in biological tissue, the wave amplitudes get attenuated and their phases are shifted. The imager measures the perturbations of these attenuations and phase delays to recalculate the optical properties of the target.

the brain function. The absorption of near-infrared waves is related to the oxygen saturation [258], the hemoglobin concentration and the water concentration of tissue [259]. The increased hemoglobin concentration in cancerous tissue results in a significant contrast compared to healthy tissue [260, 261], enabling the localization of the tumor. In addition, the measured oxygenation can also be an indicator for the likelihood of metastases [262] as well as for the success of surgery or radiation therapy [263]. In NIR spectroscopy the temporal changes in oxy- and deoxy-hemoglobin concentration can be used, e.g., to monitor the brain function or to detect hematomas [264–270].

Based on the variety of wavelengths and their compact size, diode laser NIR imaging can also be combined with the treatment of cancer. One example is interstitial photo-dynamic therapy, which is preferably carried out using diode lasers [271]. In one approach, diode lasers at different wavelengths were used to initiate photo-dynamic therapy and to monitor the photo-sensitizer fluorescence intensity, the light fluence dose distribution and changes in the blood oxygen saturation [272]. Such an on-line dosimetry allows optimizing the light delivery and therefore the outcome of the treatment [273–275].

Non-invasive, diffuse near-infrared spectroscopy and imaging are well established procedures in, e.g., cancer detection and brain studies. Based on compact and low-cost diode lasers with multiple available wavelengths, they can assist traditional diagnostics or even be combined with them [276], without adding to their size or complexity.

8. Diode laser systems emitting continuous wave terahertz radiation

There exists a frequency range within the electromagnetic spectrum that is difficult to cover directly by electronic or optical devices, but has a high potential for several applications. Due to the high absorption in water-rich samples, frequencies between 0.3–10 THz have a high application potential within the biomedical field [277]. Since histological changes in tissues are in most cases connected to changes in the water content, measuring the water volume distribution within a sample can help to distinguish between healthy and diseased tissue [278].

One way to generate terahertz radiation is to focus a femtosecond pulse onto a photo-conducting antenna converting the optical pulse into a fast broadband terahertz signal. Typical lasers are Ti:S lasers, based on a complex design and very expensive, or mode-locked diode lasers. The latter were presented generating 600 fs pulses [279], leading to a broadband spectrum up to 1.4 THz [280]. Within the biomedical field such pulsed terahertz sources have been used for the in-vitro detection of skin cancer, breast tumors or colon cancer [281–286]. The images showed a statistically significant contrast between cancerous and noncancerous tissue, resulting from differences in the water distribution and tissue structure.

A less expensive and more efficient approach towards terahertz radiation is the generation of CW-terahertz emission by photomixing of wavelength stabilized diode lasers. This technique is based on the superposition of two distinct frequencies on a photo-conducting antenna, resulting in a distinct difference frequency in the terahertz range [287]. With the wavelength being tunable by changing the injection current or the laser temperature, such systems even enable tunable terahertz emission [288].

However, combining the emission of two diode lasers is critical and may introduce additional losses within the system. Therefore, different groups have been working on compact two-color diode laser systems using monolithic approaches with Y-shaped waveguides or separate DFB sections, as well as external cavity schemes [287–292]. The first biomedical application of such diode laser based CW systems has been imaging of a human liver with metastasis [7]. Other groups confirmed that CW-terahertz radiation represents a feasible alternative to pulsed systems in distinguishing between healthy and cancerous tissues [286, 293].

A drawback of two-color lasers is the information being specific for only one wavelength. In order to reduce the time of an analysis involving multiple frequencies, different groups have been working on broadband, CW-terahertz systems. In one approach, the external cavity was extended by an additional lens focusing light diffracted by an external grating onto a structured mirror [292]. While that mirror enabled the selection of specific wavelengths for two-color systems, it could also be switched to feed multiple spectral components back to the diode (Fig. 13). In a terahertz setup this laser generated a broadband emission of 0.6 THz. In another approach even a bandwidth of 1 THz was generated [294]. These results clearly show the potential of CW diode lasers generating broadband terahertz radiation in comparison to more complicated pulsed systems.

Compared to competing systems, diode lasers are preferred choices in order to realize very compact and low-cost THz systems with sufficient output power for, e.g., spectroscopic analysis. On one hand, mode-locking of multiple longitudinal modes leads to short pulses as required for the generation of pulsed, broadband terahertz waves. On the other hand, the same lasers in CW operation enable the generation of either distinct or broadband terahertz emission in an even simpler, robust and efficient manner.

9. Outlook

Diode lasers enable a huge variety of biomedical applications, including photocoagulation, OCT imaging, diffuse optical imaging and spectroscopy, fluorescence microscopy and terahertz spectroscopy. All of these procedures either rely on the provided output power, potentially delivered in a nearly diffraction-limited beam, or other advantageous aspects such as the broadband gain for tuning purposes or the fact that the laser emission can be controlled accurately by the injection current.
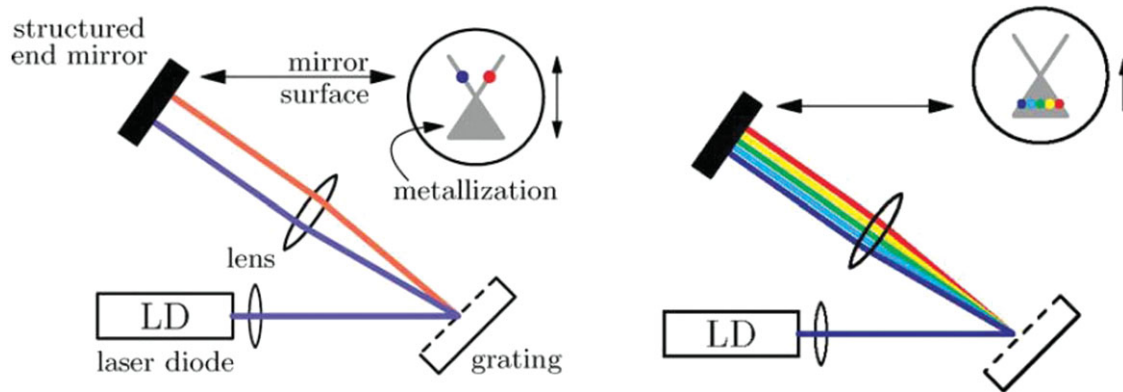
Figure 13 (online color at: www.lpr-journal.org) Fourier transform external cavity diode laser. The structured mirror enables a selection of specific wavelengths for two-color THz systems (left), as well as broadband emission when multiple spectral components are fed back to the diode (right). The figures are printed with permission from [292].

High-power diode lasers already represent a viable alternative to established systems in dermatology, dentistry, laser surgery and in cosmetic procedures, such as hair removal. The ongoing and continued development of diode lasers will lead to even higher output powers with possibly higher central lobe power. This will further increase the importance of diode lasers within the biomedical field, covering not only multiple wavelength ranges but also higher power levels.

In addition, the increased output power, especially of near-infrared diode lasers with good beam quality, will enhance the available output power in the visible range, obtained by frequency conversion. Furthermore, the development of new laser structures will lead to new emission wavelengths, e.g., in the yellow spectral range, having a strong application potential in the biomedical field. In contrast to these high-power devices, the development of GaN based diodes will at some point lead to an enhanced performance and will have a strong effect on the size and costs of visible diode laser systems for any kinds of applications.

Swept-source OCT has become an important imaging modality for biomedical applications, and due to its inherent advantages it is generally preferred compared to spectrometer-based OCT. This successful development was enabled exclusively by diode laser technology. No other gain media than semiconductors can fulfill the unique requirement for ultra-rapidly broadband tunable light sources. Whereas very compact high-speed external-cavity tunable lasers have become available during the past few years, the most recent trend goes towards monolithic edge-emitting or surface-emitting diode lasers with integrated tuning mechanism. These new technologies will drive the development of the next generation of OCT systems with improved performance and reduced cost.

One major task regarding the future development of diode laser sources will probably be the realization of very compact systems exploiting micro system technology. This was already demonstrated for frequency converted diode lasers and to some extent for amplified pulsed diode lasers. A further reduction will improve the position of diode lasers not only in biomedical applications but also in other areas. Furthermore, the approach towards more compact diode laser systems has a large potential when it comes to portable diagnostic systems for home use.

André Müller received his M. Eng. degree in Applied Physics / Medical Engineering in 2008 at the University of Applied Sciences in Berlin. In his thesis he focused on the development of compact diode laser systems for spectroscopic applications. In 2009 he joined the group of Paul Michael Petersen at the Technical University of Denmark and became a PhD student in 2010. His current research interests are the development of diode laser systems based on nonlinear frequency conversion for biomedical applications.
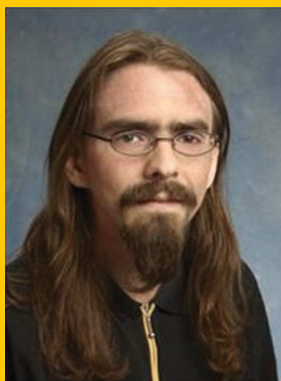
Sebastian Marschall studied at the Technical University of Darmstadt, Germany, and received his Diplom in Engineering Physics in 2008. He conducted his final project on frequency-swept laser light sources for optical coherence tomography externally at the Technical University of Denmark. In 2008, he joined the group of Prof. Peter E. Andersen at the Technical University of Denmark to continue his research on swept sources as part of the European Union project FUN OCT (FP7 Health), and received his Ph.D. degree in 2012.
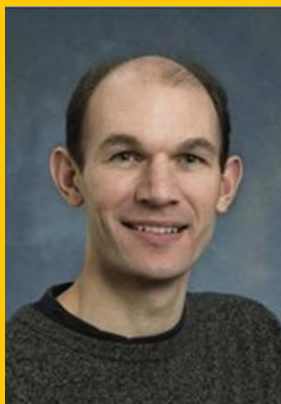
Ole Bjarlin Jensen received his M.Sc. Eng. Appl. Phys. degree in 1999 and the Ph.D. degree in 2002 from the Technical University of Denmark. His thesis concerned diode pumped solid state lasers and nonlinear frequency conversion using OPOs, SHG and SFG. In 2004 he joined the Risø National Laboratory and in 2007 the Technical University of Denmark, where he is currently senior researcher at DTU Fotonik. His current research interests include diode lasers, solid state lasers and nonlinear frequency conversion as well as biomedical applications of laser systems.
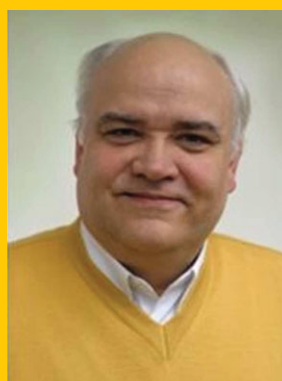
Jörg Fricke received his Diplom in physics from the University of Rostock in 1991, and the Doctor Engineer degree from the Technical University of Berlin, Berlin, Germany, in 1996. His work was focused on the development of micromechanical accelerometers in silicon surface micromachining technology. From 1997 to 1998, he worked in the field of self-organized structures on GaAs at the Paul-Drude-Institut, Berlin. Since 1998 he is dealing with the technology of laser diode manufacturing at the Ferdinand-Braun-Institut, Berlin, Germany.

Hans Wenzel received his Diplom and Doctoral degrees in physics from Humboldt-University, Berlin, Germany, in 1986 and 1991, respectively. His thesis dealt with the electro-optical modeling of semiconductor lasers. From 1991 to 1994, he was involved in a research project on the three-dimensional simulation of DFB lasers. In 1994, he joined the Ferdinand-Braun-Institut für Höchstfrequenztechnik, Berlin, Germany, where he is engaged in the development of high-brightness semiconductor lasers. His main research interests include the analysis, modeling, and simulation of optoelectronic devices.

Bernd Sumpf received his Diplom in Physics in 1981 and the Ph.D. degree in 1987 from the Humboldt-Universität zu Berlin for his work on lead salt diode lasers for spectroscopic applications. From 1993 till 1997 he worked at the Technische Universität Berlin on high-resolution spectroscopy and non-linear optics and received in 1997 the postdoctoral lecture qualification. Since 2000 he is at the Ferdinand-Braun-Institut Berlin. His current research topics are high-brightness diode lasers and diode lasers for sensory applications and RAMAN spectroscopy.

Peter E. Andersen received his MSc.E.E. in 1991 and his Ph.D. in 1994 from the Technical University of Denmark. Dr. Andersen is Senior Scientist and Research Professor at the Technical University of Denmark, where he leads the research within biomedical optics. He has more than 15 years of research experience with light sources for biomedical optics and optical coherence tomography systems and their application. Dr. Andersen has coordinated several European research programs. He has authored or co-authored more than 100 scientific publications in the above-mentioned fields, respectively. Dr. Andersen is appointed Deputy Editor of Optics Letters and editorial board member of Journal of Biophotonics.

References

[1] T. H. Maiman, Nature **187**, 493–494 (1960).

[2] A. Knigge, G. Erbert, J. Jonsson, W. Pittroff, R. Staske, B. Sumpf, M. Weyers, and G. Tränkle, Electron. Lett. **41**, 250–251 (2005).

[3] M. Kanskar, T. Earles, T. Goodnough, E. Stiers, D. Botez, and L. Mawst, Electron. Lett. **41**, 245–247 (2005).

[4] R. C. Youngquist, S. Carr, and D. E. N. Davies, Opt. Lett. **12**, 158–160 (1987).

[5] K. W. Berndt, I. Gryczynski, and J. R. Lakowicz, Rev. Sci. Instrum. **61**, 1816–1820 (1990).

[6] L. V. Wang and H. Wu, Biomedical Imaging: Principles and Imaging. (Wiley, New Jersey, 2007), chap. 11, pp. 249–281.

[7] T. Kleine-Ostmann, P. Knobloch, M. Koch, S. Hoffmann, M. Breede, M. Hofmann, G. Hein, K. Pierz, M. Sperling, and K. Donhuijsen, Electron. Lett. **37**, 1461–1463 (2001).

[8] F. F. M. de Mul, J. van Spijker, D. van der Plas, J. Greve, J. G. Aarnoudse, and T. M. Smits, Appl. Opt. **23**, 2970–2973 (1984).

[9] J. F. Brennan, Y. Wang, R. R. Dasari, and M. S. Feld, Appl. Spectrosc. **51**, 201–208 (1997).

[10] C. A. Puliafito, T. F. Deutsch, J. Boll, and K. To, Arch. Ophthalmol. **105**, 424–427 (1987).

[11] T. J. Dougherty, Sem. Surg. Oncol. **5**, 6–16 (1989).

[12] L. Longo, S. Evangelista, G. Tinacci, and A. G. Sesti, Las. Surg. Med. **7**, 444–447 (1987).

[13] G. Erbert and R. März, in: F. Bachmann, P. Loosen, and R. Poprawe (eds.), High Power Diode Lasers: Technology and Applications. (Springer, Berlin, 2007), chap. 2.1, pp. 5–7.

[14] G. V. Agrawal and N. K. Dutta, Semiconductor Lasers 2nd Edition (Van Nostrand Reinhold, New York, 1993), chap. 6.3.2, pp. 242–250.

[15] G. V. Agrawal and N. K. Dutta, Semiconductor Lasers 2nd Edition (Van Nostrand Reinhold, New York, 1993), chap. 7, pp. 319–384.

[16] M. W. Fleming and A. Mooradian, IEEE J. Quantum Electron. **17**, 44–59 (1981).

[17] K. C. Harvey and C. J. Myatt, Opt. Lett. **16**, 910–912 (1991).

[18] R. W. Boyd, Nonlinear Optics 2nd Edition (Academic Press, San Diego, 2003), chap. 1.2, pp. 4–16.

[19] B. E. A. Saleh and M. C. Teich, in: J. W. Goodman (ed.), Fundamentals of Photonics (Wiley-Interscience Publication, USA, 1991), chap. 16.2B, p. 615.

[20] A. Tünnermann, H. Zellmer, W. Schöne, A. Giesen, and K. Contag, in: R. Diehl (ed.), High Power Diode Lasers – Fundamentals, Technology, Applications, with contributions by numerous experts. (Springer, Berlin, 2000), chap. 10.1, pp. 369–373.

[21] J. A. Rossi, S. R. Chinn, J. J. Hsieh, and M. C. Finn, J. Appl. Phys. **45**, 5383–5388 (1974).

[22] H. Wenzel, F. Bugge, M. Dallmer, F. Dittmar, J. Fricke, K.-H. Hasler, and G. Erbert, IEEE Photon. Technol. Lett. **20**, 214–216 (2008).

[23] B. Sumpf, K.-H. Hasler, P. Adamiec, F. Bugge, F. Dittmar, J. Fricke, H. Wenzel, M. Zorn, G. Erbert, and G. Tränkle, IEEE J. Sel. Top. Quantum Electron. **15**, 1009–1020 (2009).

[24] K. Paschke, S. Einfeldt, A. Ginolas, K. Häusler, P. Ressel, B. Sumpf, H. Wenzel, and G. Erbert, Conference on Lasers and Electro-Optics (CLEO), CMN4 (2008).

[25] W. Pittroff, G. Erbert, B. Eppich, C. Fiebig, K. Vogel, and G. Tränkle, IEEE Trans. Compon. Packag. Technol. **33**, 206–214 (2010).

[26] L. Goldberg, H. F. Taylor, J. F. Weller, and D. R. Scifres, Appl. Phys. Lett. **46**, 236–238 (1985).

[27] P. Unger, in: R. Diehl (ed.), High Power Diode Lasers – Fundamentals, Technology, Applications, with contributions by numerous experts, (Springer, Berlin, 2000), chap. 1.4, pp. 13–15.

[28] M. Kuznetsov, F. Hakimi, R. Sprague, and A. Mooradian, IEEE Photon. Technol. Lett. **9**, 1063–1065 (1997).

[29] W. J. Alford, T. D. Raymond, and A. A. Allerman, J. Opt. Soc. Am. B **19**, 663–666 (2002).

[30] P.-T. Ho, L. A. Glasser, E. P. Ippen, and H. A. Haus, Appl. Phys. Lett. **33**, 241–242 (1978).

[31] M. B. Flynn, L. O'Faolain, and T. F. Krauss, J. Opt. Soc. Am. B **22**, 792–795 (2005).

[32] C. Lin, P. L. Liu, T. C. Darnell, D. J. Eilenberger, and R. L. Hartman. Electron. Lett. **16**, 600–602 (1980).

[33] J. Ohtsubo, Semiconductor Lasers – Stability, Instability and Chaos 2nd Enlarged Edition (Springer, Berlin, 2007), chap. 5.1.4, pp. 93–95.

[34] D. J. Derickson, R. J. Helkey, A. Mar, J. R. Karin, J. G. Wasserbauer, and J. E. Bowers, IEEE J. Quantum Electron. **28**, 2186–2202 (1992).

[35] S. Schwertfeger, A. Klehr, T. Hoffmann, A. Liero, H. Wenzel, and G. Erbert, Appl. Phys. B **103**, 603–607 (2011).

[36] I. Vurgaftman, J. R. Meyer, and L. R. Ram-Mohan, J. Appl. Phys. **89**, 5815–5875 (2001).

[37] M. Kneissl and J. Rass, in: H. Weber, P. Loosen and R. Poprawe (eds.), Landolt-Börnstein – Laser Physics and Applications, Subvolume B: Laser Systems Part 3 (Springer, Berlin, 2011), pp. 27–42.

[38] K. Iga, IEEE J. Sel. Top. Quantum Electron. **6**, 1201–1215 (2000).

[39] H. Wenzel, in: W. Schulz, H. Weber, R. Poprawe (eds.), Landolt-Börnstein – Laser Physics and Applications, Subvolume B: Laser Systems Part 2 (Springer, Berlin, 2008), chap. 5.2, pp. 163–183.

[40] R. D. Dupuis, J. Cryst. Growth **55**, 213–222 (1981).

[41] S. Nakamura, Y. Harada and M. Seno, Appl. Phys. Lett. **58**, 2021–2023 (1991).

[42] L. J. Mawst, A. Bhattacharya, M. Nesnidal, J. Lopez, D. Botez, A. V. Syrbu, V. P. Yakovlev, G. I. Suruceanu, A. Z. Mereutza, M. Jansen, and R. F. Nabiev, J. Cryst. Growth **170**, 383–389 (1997).

[43] F. Bugge, M. Zorn, U. Zeimer, A. Pietrzak, G. Erbert, and M. Weyers, J. Cryst. Growth **311**, 1065–1069 (2009).

[44] T. Onishi, K. Inoue, K. Onozawa, T. Takayama, and M. Yuri, IEEE J. Quantum Electron. **40**, 1634–1638 (2004).

[45] C. Skierbiszewski, P. Wiśniewski, M. Siekacz, P. Perlin, A. Feduniewicz-Zmuda, G. Nowak, I. Grzegory, M. Leszczyński, and S. Porowski, Appl. Phys. Lett. **88**, 221108 (2006).

[46] L. Toikkanen, M. M. Dumitrescu, A. Tukiainen, S. Viitala, M. Suominen, V. Erojärvi, V. Rimpilinen, R. Rönkkö, and M. Pessa, Proc. SPIE **5452**, 199–205 (2004).

[47] E. S. Knitter, J. N. Walpole, S. R. Chinn, C. A. Wang, and L. J. Missaggia, IEEE Phot. Technol. Lett. **5**, 605–608 (1993).

[48] J. N. Walpole, Opt. Quantum Electron. **28**, 623–645 (1996).

[49] M. Mikulla, P. Chazan, A. Schmitt, S. Morgott, A. Wetzel, M. Walther, R. Kiefer, W. Pletschen, J. Braunstein, G. Weimann, IEEE Phot. Technol. Lett. **11**, 654–656 (1998).

[50] J. P. Donelly, J. Walpole, S. H. Groves, R. J. Bailey, L. J. Missaggia, A. Napoleone, R. E. Reeder, and C. C. Cook, IEEE Phot. Technol. Lett. **10**, 1377–1379 (1998).

[51] H. Wenzel, B. Sumpf, and G. Erbert, Comptes Rendus Physique **4**, 649–661 (2003).

[52] N. Michel, M. Krakowski, I. Hassiaoui, M. Calligaro, M. Lecomte, O. Parillaud, P. Weinmann, C. Zimmermann, W. Kaiser, M. Kamp, A. Forchel, E. M. Pavelescu, J. P. Reithmaier, B. Sumpf, G. Erbert, M. Kelemen, R. Ostendorf, J.-M. García-Tijero, H. Odriozola, and I. Esquivias, Proc. SPIE **6909**, 690918 (2008).

[53] P. Crump, O. Brox, F. Bugge, J. Fricke, C. Schultz, M. Spreemann, B. Sumpf, H. Wenzel, and G. Erbert, in: J. J. Coleman, A. C. Bryce, C. Jagadish (eds.), Semiconductors and Semimetals Volume 86, Advances in Semiconductor Lasers (Academic Press, Burlington, 2012), chap. 2, pp. 49–91.

[54] H. Wenzel, A. Klehr, M. Braun, F. Bugge, G. Erbert, J. Fricke, A. Knauer, M. Weyers, and G. Tränkle, Electron. Letters, **40**, 123–124 (2004).

[55] K. Inoguchi, H. Kudo, S. Sugahara, S. Ito, H. Yagi, and H. Takiguchi, Jpn. J. Appl. Phys. **33**, 852–855 (1994).

[56] N. A. Morris, J. C. Connolly, R. U. Martinelli, J. H. Abeles, and A. L. Cook, IEEE Phot.Technol. Lett. **7**, 455–457 (1995).

[57] M. Kanskar, Y. He, J. Cai, C. Galstad, S. H. Macomber, E. Stiers, D. Botez, and L. J. Mawst, Electron. Lett. **42**, 1455–1457 (2006).

[58] Y. He, H. An, J. Cai, C. Galstad, S. Macomber, and M. Kanskar, Electron. Lett. **45**, 163–164 (2009).

[59] C. M. Schultz, P. Crump, H. Wenzel, O. Brox, A. Maaßdorf, G. Erbert, and G. Tränkle, Electron. Lett. **46**, 580–581 (2010).

[60] J. S. Major and D. F. Welch, Electron. Lett. **29**, 2121–2122 (1993).

[61] L. Hofmann, A. Klehr, F. Bugge, H. Wenzel, V. Smirnitski, J. Sebastian, and G. Erbert, Electron. Letters **36**, 534–535 (2000).

[62] M. Radziunas, K.-H. Hasler, B. Sumpf, T. Q. Tien, and H. Wenzel, J. Phys. B: At. Mol. Opt. Phys. **44**, 105401 (2011).

[63] J. Fricke, H. Wenzel, M. Matalla, A. Klehr, and G. Erbert, Semicond. Sci. Technol. **20**, 1149–1152 (2005).

[64] M. Gasser and E. E. Latta, U.S. Patent 5 144 634 (1992).

[65] C. Silfvenius, P. Blixt, C. Lindström, and A. Feitisch, Laser Focus World **39**, 69–73 (2003).

[66] P. Ressel, G. Erbert, U. Zeimer, K. Häusler, G. Beister, B. Sumpf, A. Klehr, G. Tränkle, IEEE Phot. Technol. Lett. **17**, 962–964 (2005).

[67] W. Both and J. Piprek, J. Therm. Anal. **36**, 1441–1456 (1990).

[68] W. Pittroff, G. Erbert, G. Beister, F. Bugge, A. Klein, A. Knauer, J. Maege, P. Ressel, J. Sebastian, R. Staske, and G. Tränkle, IEEE Trans. Adv. Packag. **24**, 434–441 (2001).

[69] J. J Hughes, D. B. Gilbert, and F. Z. Hawrylo, RCA Rev. **46**, 200–213 (1985).

[70] R. W. Solarz, M. A. Emanuel, J. A. Skidmore, B. L. Freitas, and W. F. Krupke, Laser Phys. **8**, 737–740 (1998).

[71] S. Weiß, E. Zabel, and H. Reichl, IEEE Trans. Comp. Packag Manufact. Technol. A **19**, 46–53 (1996).

[72] B. Sumpf and K. Häusler, in: H. Weber, P. Loosen and R. Poprawe (eds.), Landolt-Börnstein – Laser Physics and Applications, Subvolume B: Laser Systems Part 3 (Springer, Berlin, 2011), pp. 155–173.

[73] B. Sumpf and U. Zeimer, in: H. Weber, P. Loosen and R. Poprawe (eds.), Landolt-Börnstein – Laser Physics and Applications, Subvolume B: Laser Systems Part 3 (Springer, Berlin, 2011), pp. 174–182.

[74] http://www.nichia.co.jp/en/product/laser_main.html

[75] C. Sasaoka, K. Fukuda, M. Ohya, K. Shiba, M. Sumino, S. Kohmoto, K. Naniwae, M. Matsudate, E. Mizuki, I. Masumoto, R. Kobayashi, K. Kudo, T. Sasaki and K. Nishi, Phys. Stat. Sol. A **203**, 1824–1828 (2006).

[76] http://www.nlight.net/nlight-files/file/datasheets/ Single%20emitters/nLIGHT_C-Mount_630– 690nm_052312.pdf

[77] B. Sumpf, M. Zorn, R. Staske, J. Fricke, P. Ressel, A. Ginolas, K. Paschke, G. Erbert, M. Weyers, and G. Tränkle, IEEE J. Sel. Top. Quantum Electron. **13**, 1188–1193 (2007).

[78] B. Sumpf, M. Zorn, M. Maiwald, R. Staske, J. Fricke, P. Ressel, G. Erbert, M. Weyers, and G. Tränkle, Phot. Technol. Lett. **20**, 575–577 (2008).

[79] B. Sumpf, G. Beister, G. Erbert, J. Fricke, A. Knauer, W. Pittroff, P. Ressel, J. Sebastian, H. Wenzel, and G. Tränkle, Electron. Lett. **37**, 351–353 (2001).

[80] http://www.axcelphotonics.com/808MM.php

[81] H. Taniguchi, H. Ishii, R. Minato, Y. Ohki, T. Namegaya, and A. Kasukawa, IEEE J. Sel. Top. Quant. Electron. **13**, 1176–1179 (2007).

[82] P. Crump, G. Blume, K. Paschke, R. Staske, A. Pietrzak, U. Zeimer, S. Einfeldt, A. Ginolas, F. Bugge, K. Häusler, P. Ressel, H. Wenzel, and G. Erbert, Proc. SPIE **7198**, 719814 (2009).

[83] F. Bugge, G. Erbert, J. Fricke, S. Gramlich, R. Staske, H. Wenzel, U. Zeimer, and M. Weyers, Appl. Phys. Lett. **79**, 1965 (2001).

[84] A. Avramescu, T. Lermer, J. Müller, C. Eichler, G. Bruederl, M. Sabathil, S. Lutgen, and U. Strauss, Appl. Phys. Express **3**, 061003 (2010).

[85] J. W. Raring, M. C. Schmidt, C. Poblenz, Y.-C. Chang, M. J. Mondry, B. Li, J. Iveland, B. Walters, M. R. Krames, R. Craig, P. Rudy, J. S. Speck, S. P. DenBaars, and S. Nakamura, Appl. Phys. Express **3**, 112101 (2010).

[86] C. Vierheilig, C. Eichler, S. Tautz, A. Lell, J. Müller, F. Kopp, B. Stojetz, T. Hager, G. Brüderl, A. Avramescu, T. Lermer, J. Ristic, and U. Strauss, Proc. SPIE **8277**, 82770K (2012).

[87] S. Takagi, Y. Enya, T. Kyono, M. Adachi, Y. Yoshizumi, T. Sumitomo, Y. Yamanaka, T. Kumano, S. Tokuyama, K.

Sumiyoshi, N. Saga, M. Ueno, K. Katayama, T. Ikegami, T. Nakamura, K. Yanashima, H. Nakajima, K. Tasai, K. Naganuma, N. Fuutagawa, Y. Takiguchi, T. Hamaguchi, and M. Ikeda, Appl. Phys. Express **5**, 082102 (2012).

[88] G. Blume, D. Feise, C. Kaspari, A. Sahm, and K. Paschke, Proc. SPIE **8280**, 82800E (2012).

[89] P. Adamiec, B. Sumpf, I. Rüdiger, J. Fricke, K.-H. Hasler, P. Ressel, H. Wenzel, M. Zorn, G. Erbert, and G. Tränkle, Opt. Lett. **34**, 2456–2458 (2009).

[90] C. Kaspari, G. Blume, D. Feise, K. Paschke, G. Erbert, and M. Weyers, IET Optoelectron. **5**, 121–127 (2011).

[91] B. Sumpf, P. Adamiec, M. Zorn, H. Wenzel, and G. Erbert, IEEE Phot. Technol. Lett. **23**, 266–268 (2011).

[92] G. Erbert, J. Fricke, R. Hülsewede, A. Knauer, W. Pittroff, P. Ressel, J. Sebastian, B. Sumpf, H. Wenzel, and G. Tränkle, Proc. SPIE **4995**, 29–38 (2003).

[93] F. Dittmar, B. Sumpf, J. Fricke, G. Erbert, and G. Tränkle, IEEE Phot. Technol. Lett. **18**, 601–603 (2006).

[94] C. Fiebig, G. Blume, C. Kaspari, D. Feise, J. Fricke, M. Matalla, W. John, H. Wenzel, K. Paschke, and G. Erbert, Electron. Letters **44**, 1253–1255 (2008).

[95] B. Sumpf, K.-H. Hasler, P. Adamiec, F. Bugge, J. Fricke, P. Ressel, H. Wenzel, G. Erbert, and G. Tränkle, Proc SPIE **7230**, 72301E (2009).

[96] J. Mobley and T. Vo-Dinh, in: T. Vo-Dinh (ed.), Biomedical Photonics Handbook (CRC Press, Boca Raton, 2003), chap. 2.2, pp. 22–31.

[97] J. Mobley and T. Vo-Dinh, in: T. Vo-Dinh (ed.), Biomedical Photonics Handbook (CRC Press, Boca Raton, 2003), chap. 2.4, pp. 55–89.

[98] A. Kim and B. C. Wilson, in: A. J. Welch and M. J. C. van Gemert (eds.), Optical-thermal Response of Laser-irradiated Tissue 2nd edition (Springer, New York, 2011), chap 8.2.2.1, pp. 279–286.

[99] A. Vogel and V. Venugopalan, Chem. Rev. **103**, 577–644 (2003).

[100] R. R. Anderson and J. A. Parrish, Lasers Surg. Med. **1**, 263–276 (1981).

[101] V. V. Tuchin, in: T. Vo-Dinh (ed.), Biomedical Photonics Handbook (CRC Press, Boca Raton, 2003), chap. 3.3.1, pp. 105–107.

[102] V. Vejjabhinanta, K. Nouri, A. Singh, R. Huo, and R. Charoensawad, in: K. Nouri (ed.), Lasers in Dermatology and Medicine (Springer, London, 2011), chap. 8, pp. 91–102.

[103] R. Wanitphakdeedecha and T. S. Alster, in: K. Nouri (ed.), Lasers in Dermatology and Medicine (Springer, London, 2011), chap. 9, pp. 103–122.

[104] D. Michael and S. Kilmer, in: K. Nouri (ed.), Lasers in Dermatology and Medicine (Springer, London, 2011), chap. 3, pp. 33–44.

[105] T. Meier, B. Willke, and K. Danzmann, Opt. Lett. **35**, 3742–3744 (2010).

[106] S. Konno, T. Kojima, S. Fujikawa, and K. Yasui, Opt Lett. **25**, 105–107 (2000).

[107] R. J. Min, S. E. Zimmet, M. N. Isaacs, and M. D. Forrestal, J. Vasc. Interv. Radiol. **12**, 1167–1171 (2001).

[108] T. Passeron, V. Olivier, L. Duteil, F. Desruelles, E. Fontas, and J.-P. Ortonne, J. Am. Acad. Dermatol. **48**, 768–774 (2003).

[109] L. Navarro, R. J. Min, and C. Boné, Dermatol. Surg. **27**, 117–122 (2001).

[110] T. M. Proebstle, H. A. Lehr, A. Kargl, C. Espinola-Klein, W. Rother, S. Bethge, and J. Knop, J. Vasc. Surg. **35**, 729–736 (2002).

[111] Y. Huang, M. Jiang, W. Li, X. Lu, X. Huang, and M. Lu, J. Vasc. Surg. **42**, 494–501 (2005).

[112] X. Lu, K. Ye, W. Li, M. Lu, X. Huang, and M. Jiang, J. Vasc. Surg. **48**, 675–679 (2008).

[113] X. Lu, K. Ye, H. Shi, W. Li, Y. Huang, X. Huang, M. Lu, and M. Jiang, J. Vasc. Surg. **54**, 139–145 (2011).

[114] T. M. Proebstle, F. Krummenauer, D. Gül, and J. Knop, Dermatol. Surg. **30**, 174–178 (2004).

[115] M. Landthaler and U. Hohenleutner, Photodermatol. Photoimmunol. Photomed. **22**, 324–332 (2006).

[116] M. J. C. van Gemert, D. J. Smithies, W. Verkruysse, T. E. Milner, and J. S. Nelson, Phys. Med. Biol. **42**, 41–50 (1997).

[117] P. Kaudewitz, W. Klövekorn, and W. Rother, Dermatol. Surg. **27**, 101–106 (2001).

[118] P. Kaudewitz, W. Klövekorn, and W. Rother, Dermatol. Surg. **28**, 1031–1034 (2002).

[119] T. Passeron, V. Olivier, L. Duteil, F. Desruelles, E. Fontas, and J.-P.Ortonne, J. Am. Acad. Dermatol. **48**, (2003); 768–774.

[120] J. L. Levy and C. Berwald, J. Cosmet. Laser Ther. **6**, 217–221 (2004).

[121] M. Lapidoth, E. Yaniv, D. B. Amitai, E. Raveh, E. Kalish, M. Waner, and M. David, Dermatol. Surg. **31**, 1308–1312 (2005).

[122] F. Angiero, S. Benedicenti, A. Benedicenti, K. Arcieri, and E. Bernè, Photomed. Laser Surg. **27**, 553–559 (2009).

[123] W. J. Genovese, M. T. Botti Rodrigues dos Santos, F. Faloppa, and L. A. de Souza Merli, Photomed. Laser Surg. **28**, 147–151 (2009).

[124] C. Fornaini, J. P. Rocca, M. F. Bertrand, E. Merigo, S. Nammour, and P. Vescovi, Photomed. Laser Surg. **25**, 381–392 (2007).

[125] G. Wendt-Nordahl, S. Huckele, P. Honeck, P. Alken, T. Knoll, M. S. Michel, and A. Häcker, Eur. Urol. **52**, 1723–1728 (2007).

[126] F. Angiero, L. Parma, R. Crippa, and S. Benedicenti, Lasers Med. Sci. **27**, 383–388 (2012).

[127] G. Romanos and G.-H. Nentwig, J. Clin. Laser Med. Surg. **17**, 193–197 (1999).

[128] D. Huang, E.A. Swanson, C.P. Lin, J.S. Schuman, W.G. Stinson, W. Chang, M.R. Hee, T. Flotte, K. Gregory, C.A. Puliafito, and J.G. Fujimoto, Science **254**, 1178–1181 (1991).

[129] S. Marschall, B. Sander, M. Mogensen, T. M. Jørgensen, and P. E. Andersen, Anal. Bioanal. Chem. **400**, 2699–2720 (2011).

[130] D. Stifter, Appl. Phys. B **88**, 337–357 (2007).

[131] A. F. Fercher, C. K. Hitzenberger, G. Kamp, and S. Y. El-Zaiat, Opt. Comm. **117**, 43–48 (1995).

[132] U. Haberland, W. Rütten, V. Blazek, and H. J. Schmitt, Proc. SPIE **2389**, 503–512 (1995).

[133] S. R. Chinn, E. A. Swanson, and J. G. Fujimoto, Opt. Lett. **22**, 340–342 (1997).

[134] B. Golubovic, B. E. Bouma, G. J. Tearney, and J. G. Fujimoto, Opt. Lett. **22**, 1704–1706 (1997).

[135] B. Potsaid, B. Baumann, D. Huang, S. Barry, A. E. Cable, J. S. Schuman, J. S. Duker, and J. G. Fujimoto, Opt. Express **18**, 20029–20048 (2010).

[136] S. H. Yun, G. J. Tearney, J. F. de Boer, and B. E. Bouma, Opt. Express **12**, 2977–2998 (2004).

[137] W. Wieser, B. R. Biedermann, T. Klein, C. M. Eigenwillig, and R. Huber, Opt. Express **18**, 14685–14704 (2010).

[138] T. Klein, W. Wieser, R. André, T. Pfeiffer, C. M. Eigenwillig, and R. Huber, Proc. SPIE **8213**, 82131E (2012).

[139] S. H. Yun, C. Boudoux, G. J. Tearney, and B. E. Bouma, Opt. Lett. **28**, 1981–1983 (2003).

[140] M. A. Choma, K. Hsu, and J. A. Izatt, J. Biomed. Opt. **10**, 044009 (2005).

[141] B. R. Biedermann, W. Wieser, C. M. Eigenwillig, T. Klein, and R. Huber, Opt. Express **17**, 9947–9961 (2009).

[142] D. C. Adler, W. Wieser, F. Trepanier, J. M. Schmitt, and R. A. Huber, Opt. Express **19**, 20930–20939 (2011).

[143] V. Jayaraman, J. Jiang, B. Potsaid, G. Cole, J. G. Fujimoto, and A. Cable, Proc. SPIE **8276**, 82760D (2012).

[144] M. P. Minneman, J. Ensher, M. Crawford, and D. Derickson, Proc. SPIE **8311**, 831116 (2011).

[145] F. D. Nielsen, L. Thrane, J. Black, K. Hsu, A. Bjarklev, and P. E. Andersen, Proc. SPIE **5861**, 58610H (2005).

[146] M. K. Harduar, A. Mariampillai, B. Vuong, K. H. Y. Cheng, L. R. Chen, X. Gu, B. A. Standish, and V. X. D. Yang, Proc. SPIE **7580**, 75802S (2010).

[147] B. R. Biedermann, W. Wieser, C. M. Eigenwillig, G. Palte, D. C. Adler, V. J. Srinivasan, J. G. Fujimoto, and R. Huber, Opt. Lett. **33**, 2556–2558 (2008).

[148] T. Klein, W. Wieser, C. M. Eigenwillig, B. R. Biedermann, and R. Huber, Opt. Express **19**, 3044–3062 (2011).

[149] S. Marschall, T. Klein, W. Wieser, T. Torzicky, M. Pircher, B. R. Biedermann, C. Pedersen, C. K. Hitzenberger, R. Huber, and P. E. Andersen, Proc. SPIE **8213**, 82130R (2012).

[150] S. Marschall, C. Pedersen, and P. E. Andersen, Biomed. Opt. Express **3**, 1620–1631 (2012).

[151] B. D. Goldberg, S. M. R. M. Nezam, P. Jillella, B. E. Bouma, and G. J. Tearney, Opt. Express **17**, 3619–3629 (2009).

[152] M. Kuznetsov, W. Atia, B. Johnson, and D. Flanders, Proc. SPIE **7554**, 75541F (2010).

[153] K. Totsuka, K. Isamoto, T. Sakai, A. Morosawa, and C. Chong, Proc. SPIE **7554**, 75542Q (2010).

[154] R. Huber, M. Wojtkowski, K. Taira, J. G. Fujimoto, and K. Hsu, Opt. Express **13**, 3513–3528 (2005).

[155] R. Huber, M. Wojtkowski, and J. G. Fujimoto, Opt. Express **14**, 3225–3237 (2006).

[156] W. Y. Oh, B. J. Vakoc, M. Shishkov, G. J. Tearney, and B. E. Bouma, Opt. Lett. **35**, 2919–2921 (2010).

[157] B. Potsaid, V. Jayaraman, J. G. Fujimoto, J. Jiang, P. J. S. Heim, and A. E. Cable, Proc. SPIE **8213**, 82130M (2012).

[158] V. Jayaraman, J. Jiang, H. Li, P. Heim, G. Cole, B. Potsaid, J. G. Fujimoto, and A. Cable, Conference on Lasers and Electro-Optics (CLEO), PDPB2 (2011).

[159] M. K. K. Leung, A. Mariampillai, B. A. Standish, K. K. Lee, N. R. Munce, I. A. Vitkin, and V. X. D. Yang, Opt. Lett. **34**, 2814–2816 (2009).

[160] S. Marschall, T. Klein, W. Wieser, B. R. Biedermann, K. Hsu, K. P. Hansen, B. Sumpf, K.-H. Hasler, G. Erbert, O. B. Jensen, C. Pedersen, R. Huber, and P. E. Andersen, Opt. Express **18**, 15820–15831 (2010).

[161] F. D. Nielsen, L. Thrane, K. Hsu, A. Bjarklev, and P. E. Andersen, Opt. Comm. **271**, 197–202 (2007).

[162] W. P. Risk, T. R. Gosnell, and A. V. Nurmikko, Compact Blue-Green Lasers (Cambridge University Press, Cambridge, 2003), chap. 2.3.1, pp. 43–50.

[163] G. D. Boyd and D. A. Kleinman, J. Appl. Phys. **39**, 3597 (1968).

[164] M. Übernickel, R. Güther, G. Blume, C. Fiebig, K. Paschke, and G. Erbert, Appl. Phys. B **99**, 457–464 (2010).

[165] W. P. Risk, T. R. Gosnell, and A. V. Nurmikko, Compact Blue-Green Lasers (Cambridge University Press, Cambridge, 2003), chap. 2.4, pp. 56–101.

[166] M. M. Fejer, G. A. Magel, D. H. Jundt, and R. L. Byer, IEEE J. Quantum Electron. **28**, 2631–2654 (1992).

[167] H. K. Nguyen, M. H. Hu, N. Nishiyama, N. J. Visovsky, Y. Li, K. Song, X. Liu, J. Gollier, L. C. Hughes Jr., R. Bhat, and C.-E. Zah, IEEE Photon. Technol. Lett. **18**, 682–684 (2006).

[168] M. Iwai, T. Yoshino, S. Yamaguchi, M. Imaeda, N. Pavel, I. Shoji, and T. Taira, Appl. Phys. Lett. **83**, 3659–3661 (2003).

[169] W. P. Risk, T. R. Gosnell, and A. V. Nurmikko, Compact Blue-Green Lasers (Cambridge University Press, Cambridge, 2003), chap. 4, pp. 183–222.

[170] W. P. Risk, T. R. Gosnell, and A. V. Nurmikko, Compact Blue-Green Lasers (Cambridge University Press, Cambridge, 2003), chap. 5, pp. 223–262.

[171] J. M. Yarborough, J. Falk, and C. B. Hitz, Appl. Phys. Lett. **18**, 70–73 (1971).

[172] L. K. Samanta, T. Yanagawa, and Y. Yamamoto, Opt. Comm. **76**, 250–252 (1990).

[173] L. McDonagh and R. Wallenstein, Opt. Lett. **32**, 802–804 (2007).

[174] T. Mizushima, H. Furuya, S. Shikii, K. Kosukame, K. Mizuuchi, and K. Yamamoto, Appl. Phys. Express **1**, 032003 (2008).

[175] S. Chaitanya Kumar, G. K. Samanta, K. Devi, and M. Ebrahim-Zadeh, Opt. Express **19**, 11152–11169 (2011).

[176] Y. Kaneda, J. M. Yarborough, L. Li, N. Peyghambarian, L. Fan, C. Hessenius, M. Fallahi, J. Hader, J. V. Moloney, Y. Honda, M. Nishioka, Y. Shimizu, K. Miyazono, H. Shimatani, M. Yoshimura, Y. Mori, Y. Kitaoka, and T. Sasaki, Opt. Lett. **33**, 1705–1707 (2008).

[177] G. F. Albrecht, J. M. Eggleston, and J. J. Ewing, Opt. Comm. **52**, 401–404 (1985).

[178] A. Stingl, M. Lenzner, C. Spielmann, and F. Krausz, Opt. Lett. **20**, 602–604 (1995).

[179] W. Denk, J. H. Strickler, and W. W. Webb, Science **248**, 73–76 (1990).

[180] P. D. Maker and R. W. Terhune, Phys. Rev. **137**, A801–A818 (1965).

[181] O. B. Jensen, P. E. Andersen, B. Sumpf, K.-H. Hasler, G. Erbert, and P. M. Petersen, Opt. Express **17**, 6532–6539 (2009).

[182] A. Müller, O. B. Jensen, A. Unterhuber, T. Le, A. Stingl, K.-H. Hasler, B. Sumpf, G. Erbert, P. E. Andersen, and P. M. Petersen, Opt. Express **19**, 12156 (2011).

[183] D. Jedrzejczyk, R. Güther, K. Paschke, W.-J. Jeong, H.-Y. Lee, and G. Erbert, Opt. Lett. **36**, 367–369 (2011).

[184] C. Fiebig, A. Sahm, M. Übernickel, G. Blume, B. Eppich, K. Paschke, and G. Erbert, Opt. Express **17**, 22785–22790 (2009).

[185] P. Unger, in: R. Diehl (ed.), High Power Diode Lasers – Fundamentals, Technology, Applications, with contributions by numerous experts. (Springer, Berlin, 2000), chap. 4.3, pp. 46–49.

[186] A. Müller, O. B. Jensen, K.-H. Hasler, B. Sumpf, G. Erbert, P. E. Andersen, and P. M. Petersen, Opt. Lett. **37**, 3753–3755 (2012).

[187] M.-W. Hsiung, B.-H. Kang, W.-F. Su, L. Pai, and H.-W. Wang, Ann. Otol. Rhinol. Laryngol. **112**, 534–539 (2003).

[188] Y. Kishimoto, S. Hirano, N. Kato, A. Suehiro, S.-I. Kanemaru, and J. Ito, Ann. Otol. Rhinol. Laryngol. **117**, 881–885 (2008).

[189] H. Miyazaki, J. Kato, H. Watanabe, H. Harada, H. Kakizaki, A. Tetsumura, A. Sato, and K. Omura, Oral Surg. Oral Med. Oral Pathol. Oral Radiol. Endod. **107**, 164–172 (2009).

[190] R. J. Lane, J. J. Wynne, R. G. Geronemus, Laser Surg. Med. **6**, 504–513 (1987).

[191] W. G. Telford, in: T. S. Hawley and R. G. Hawley (eds.), Methods in Molecular Biology: Flow Cytometry Protocols (Humana Press Inc., Totowa, 2004), chap. 23.2, pp. 402–410.

[192] G. Palumbo, M. Caruso, E. Crescenzi, M.F. Tecce, G. Roberti, and A. Colasanti, J. Photochem. Photobiol. B: Biol. **36**, 41–46 (1996).

[193] Y. Yuanlong, Y. Yanming, L. Fuming, L. Yufen, and M. Paozhong, Laser Surg. Med. **7**, 528–532 (1987).

[194] J. H. Lundeman, O. B. Jensen, P. E. Andersen, S. Andersson-Engels, B. Sumpf, G. Erbert, and P. M. Petersen, Opt. Express **16**, 2486–2493 (2008).

[195] H. Xie, H. Liu, P. Svenmarker, J. Axelsson, C. T. Xu, S. Gräfe, J. H. Lundeman, H. P. H. Cheng, S. Svanberg, N. Bendsoe, P. E. Andersen, K. Svanberg, and S. Andersson-Engels, J. Biomed. Opt. **16**, 066002 (2011).

[196] E. Karamehmedović, C. Pedersen, M. Thalbitzer Andersen, and P. Tidemand-Lichtenberg, Opt. Express. **15**, 12240–12245 (2007).

[197] K. Li, H. Wang, N. J. Copner, C. B. E. Gawith, I. G. Knight, H.-U. Pfeiffer, B. Musk, and G. Moss, Opt. Lett. **36**, 361–363 (2011).

[198] H. K. Choi and C. A. Wang, Appl. Phys. Lett. **57**, 321–323 (1990).

[199] M. Fallahi, L. Fan, Y. Kaneda, C. Hessenius, J. Hader, H. Li, J. V. Moloney, B. Kunert, W. Stolz, S. W. Koch, J. Murray, and R. Bedford, IEEE Photon. Technol. Lett. **20**, 1700–1702 (2008).

[200] P. A. Franken, A. E. Hill, C. W. Peters, and G. Weinreich, Phys. Rev. Lett. **7**, 118–119 (1961).

[201] H. Schneckenburger, P. Weber, T. Bruns, and M. Wagner, in: V. V. Tuchin (ed.), Handbook of Photonics for Biomedical Science (CRC Press, Boca Raton, 2010), chap. 4.2.4, pp. 122–123.

[202] M. Hammer, S. Quick, M. Klemm, S. Schenke, N. Mata, A. Eitner, and D. Schweitzer, Proc. SPIE **7183**, 71832S (2009).

[203] C.-W. Chang, M. Wu, S. D. Merajver, and M.-A. Mycek, J. Biomed. Opt. **14**, 060502 (2009).

[204] G.-J. Bakker, V. Andresen, R. M. Hoffman, and P. Friedl, Meth. Enzymol. **504**, 109–125 (2012).

[205] H.-P. Lassalle, M. Wagner, L. Bezdetnaya, F. Guillemin, and H. Schneckenburger, J. Photochem. Photobiol. B **92**, 47–53 (2007).

[206] A. V. Agronskaia, L. Tertoolen, and H. C. Gerritsen, J. Biomed. Opt. **9**, 1230–1237 (2004).

[207] Y. Sun, N. Hatami, M. Yee, M. Yee, J. Phipps, D. S. Elson, F. Gorin, R. J. Schrot, and L. Marcu, J. Biomed. Opt. **15**, 056022 (2010).

[208] S. Bloch, F. Lesage, L. McIntosh, A. Gandjbakhche, K. Liang, and S. Achilefu, J. Biomed. Opt. **10**, 054003 (2005).

[209] J. McGinty, N. P. Galletly, C. Dunsby, I. Munro, D. S. Elson, J. Requejo-Isidro, P. Cohen, R. Ahmad, A. Forsyth, A. V. Thillainayagam, M. A. A. Neil, P. M. W. French, and G. W. Stamp, Biomed. Opt. Express **1**, 627–640 (2010).

[210] C. Eggeling, L. Brand, and C. A. M. Seidel, Bioimaging **5**, 105–115 (1997).

[211] B. E. A. Saleh and M. C. Teich, in: J. W. Goodman (ed.), Fundamentals of Photonics (Wiley-Interscience Publication, USA, 1991), chap. 14.3, pp. 522–536.

[212] O. Svelto, S. Longhi, G. Della Valle, S. Kück, G. Huber, M. Pollnau, H. Hillmer, S. Hansmann, R. Engelbrecht, H. Brand, J. Kaiser, A. B. Peterson, R. Malz, S. Steinberg, G. Marowsky, U. Brinkmann, D. Lot, A. Borsutzky, H. Wächter, M. W. Sigrist, E. Saldin, E. Schneidmiller, M. Yurkov, K. Midorikawa, J. Hein, R. Sauerbrey, and J. Helmcke, in: F. Träger (ed.), Springer Handbook of Lasers and Optics (Springer Science and Business Media, New York, 2007), chap. 11.1.5, pp. 605–614.

[213] V. F. Olle, A. Wonfor, P. P. Vasilev, R. V. Penty, and I. H. White, Conference on Lasers and Electro-Optics (CLEO), JWA82 (2011).

[214] H. Wenzel, A. Klehr, S. Schwertfeger, A. Liero, Th. Hoffmann, O. Brox, M. Thomas, G. Erbert, and G. Tränkle, Proc. SPIE **8241**, 82410V (2012).

[215] T. Oki, S. Kono, M. Kuramoto, M. Ikeda, and H. Yokoyama, Appl. Phys. Express **2**, 032101 (2009).

[216] S. Kono, T. Oki, T. Miyajima, M. Ikeda, and H. Yokoyama, Appl. Phys. Lett. **93**, 121113 (2008).

[217] T. Schönau, S. M. Riecke, K. Lauritsen, and R. Erdmann, Proc. SPIE **7917**, 791707 (2011).

[218] T. Schönau, K. Lauritsen, S. M. Riecke, R. Erdmann, S. McNeil, and P. Battle, Conference on Lasers and Electro-Optics (CLEO), JThB93 (2011).

[219] Y. Liu, J. Zhang, and W. Zhao, Opt. Comm. **281**, 4971–4974 (2008).

[220] H. Wenzel, S. Schwertfeger, A. Klehr, D. Jedrzejczyk, T. Hoffmann, and G. Erbert, Opt. Lett. **37**, 1826–1828 (2012).

[221] J. C. Balzer, T. Schlauch, A. Klehr, G. Erbert, and M. R. Hofmann, Proc. SPIE **8277**, 827713 (2012).

[222] S. M. Riecke, K. Lauritsen, R. Erdmann, M. Übernickel, K. Paschke, and G. Erbert, Opt. Lett. **35**, 1500–1502 (2010).

[223] M. Kumar, C. Xia, X. Ma, V. V. Alexander, M. N. Islam, F. L. Terry Jr., C. C. Aleksoff, A. Klooster, and D. Davidson, Opt. Express **16**, 6194–6201 (2008).

[224] Y. S. Bae, D. Lee, S. Moon, Y. J. Won, and D. Y. Kim, Proc. SPIE **6443**, 64430W (2007).

[225] D. Kepshire, N. Mincu, M. Hutchins, J. Gruber, and H. Dehghani, Rev. Sci. Instrum. **80**, 043701 (2009).

[226] F. Koberling, M. Langkopf, D. Klemme, A. Bülter, V. Buschmann, K. Lauritsen, and R. Erdmann, Proc. SPIE **6860**, 68601N (2008).

[227] E. Mendez, D. S. Elson, M. Koeberg, C. Dunsby, and D. D. C. Bradley, Rev. Sci. Instrum. **75**, 1264–1267 (2004).

[228] M. S. Patterson, B. C. Wilson, and D. R. Wyman, Lasers Med. Sci. **6**, 155–168 (1991).

[229] S. R. Arridge, Phys. Med. Biol. **37**, 1531–1560 (1993).

[230] R. F. Bonner, R. Nossal, S. Havlin, and G. H. Weiss, Opt. Soc. Am. A **4**, 423–432 (1987).

[231] W. M. Star, J. P. A. Marijnissen, and J. C. Gemert, Phys. Med. Biol. **33**, 437–545 (1988).

[232] A. Yodh and B. Chance, Phys. Today **48**, 34–40 (1995).

[233] D. J. Hawrysz and E. M. Sevick-Muraca, Neoplasia **2**, 388–417 (2000).

[234] S. B. Colak, M. B. van der Mark, G. W. 't Hooft, J. H. Hoogenraad, E. S. van der Linden, and F. A. Kuijpers, IEEE J. Sel. Top. Quantum Electron. **5**, 1143–1158 (1999).

[235] M. B. van der Mark, G. W. 't Hooft, J. Chen, R. Richards-Kortum, and B. Chance, Biomedical Optical Spectroscopy and Diagnostics (BOSD), PD6 (2000).

[236] M. Cope and D. T. Delpy, Med. & Biol. Eng. & Comput. **26**, 289–294 (1988).

[237] F. E. W. Schmidt, M. E. Fry, E. M. C. Hillman, J. C. Hebden, and D. T. Delpy, Rev. Sci. Instrum. **71**, 256–265 (2000).

[238] D. Grosenick, H. Wabnitz, and H. Rinneberg, Appl. Opt. **36**, 221–231 (1997).

[239] D. Grosenick, H. Wabnitz, H. H. Rinneberg, K. T. Moesta, and P. M. Schlag, Appl. Opt. **38**, 2927–2943 (1999).

[240] M. Oda, Y. Yamashita, H. Kan, H. Miyajima, A. Nakkano, S. Suzuki, A. Suzuki, K. Shimizu, S. Muramatsu, N. Sugiura, K. Ohta, and Y. Tsuchiya, Proc. SPIE **2979**, 765–773 (1997).

[241] V. Ntziachristos, X. Ma, A. G. Yodh, and B. Chance, Rev. Sci. Instrum. **70**, 193–201 (1999).

[242] J. P Van Houten, D. A Benaron, S. Spilman, and D. K Stevenson, Pediatric Research **39**, 470–476 (1996).

[243] D. Grosenick, K. T. Moesta, H. Wabnitz, J. Mucke, C. Stroszczynski, R. Macdonald, P. M. Schlag, and H. Rinneberg, Appl. Opt. **42**, 3170–3186 (2003).

[244] B. Pogue, M. Testorf, T. McBride, U. Osterberg, and K. Paulsen, Opt. Express **1**, 391–403 (1997).

[245] H. Jiang, K. D. Paulsen, U. L. Osterberg, B. W. Pogue, and M. S. Patterson, Opt. Lett. **20**, 2128–2130 (1995).

[246] S. Fantini, M. A. Franceschini, G. Gaida, H. Jess, W. W. Mantulin, K. T. Moesta, P. M. Schlag, and M. Kaschke, Med. Phys. **23**, 149–157 (1996).

[247] M. A. Franceschini, K. T. Moesta, S. Fantini, G. Gaida, E. Gratton, H. Jess, W. W. Mantulin, M. Seeber, P. M. Schlag, and M. Kaschke, Proc. Natl. Acad. Sci. USA **94**, 6468–6473 (1997).

[248] S. Fantini, S. A. Walker, M. A. Franceschini, M. Kaschke, P. M. Schlag, and K. T. Moesta, Appl. Opt. **37**, 1982–1989 (1998).

[249] K. T. Moesta, S. Fantini, H. Jess, S. Totkas, M. A. Franceschini, M. Kaschke, and P. M. Schlag, J. Biomed. Opt. **3**, 129–136 (1998).

[250] T. O. McBride, B. W. Pogue, E. D. Gerety, S. B. Poplack, U. L. Osterberg, and K. D. Paulsen, Appl. Opt. **38**, 5480–5490 (1999).

[251] T. H. Pham, O. Coquoz, J. B. Fishkin, E. Anderson, and B. J. Tromberg, Rev. Sci. Instrum. **71**, 2500–2513 (2000).

[252] B. J. Tromberg, N. Shah, R. Lanning, A. Cerussi, J. Espinoza, T. Pham, L. Svaasand, and J. Butler, Neoplasia **2**, 26–40 (2000).

[253] N. Shah, A. Cerussi, C. Eker, J. Espinoza, J. Butler, J. Fishkin, R. Hornung, and B. Tromberg, Proc. Natl. Acad. Sci. USA **98**, 4420–4425 (2001).

[254] A. E. Cerussi, D. Jakubowski, N. Shah, F. Bevilacqua, R. Lanning, A. J. Berger, D. Hsiang, J. Butler, R. F. Holcombe, and B. J. Tromberg, J. Biomed. Opt. **7**, 60–71 (2002).

[255] S. Fantini and M. A. Franceschini, in: V. V. Tuchin (ed.), Handbook of Optical Biomedical Diagnostics (SPIE, Washington, 2002), chap. 7.1, p. 406.

[256] S. Kobayashi, Y. Yamamoto, M. Ito, and T. Kimura, IEEE J. Quantum Electron. **18**, 582–595 (1982).

[257] E. M. Sevick, B. Change, J. Leigh, S. Nioka, and M. Maris, Anal. Biochem. **195**, 330–351 (1991).

[258] F. F. Jöbsis, Science **198**, 1264–1267 (1977).

[259] B. J. Tromberg, O. Coquez, J. B. Fishkin, T. Pham, E. R. Anderson, J. Butler, M. Cahn, J. D. Gross, V. Venugopalan, and D. Pham, Philos. Trans. R. Soc. Lond. B **352**, 661–668 (1997).

[260] J. B. Fishkin, O. Coquoz, E. R. Anderson, M. Brenner, and B. J. Tromberg, Appl. Opt. **36**, 10–20 (1997).

[261] A. F. Profio and G. A. Navarro, Med. Phys. **16**, 60–65 (1989).

[262] D. M. Brizel, S. P. Scully, J. M. Harrelson, L. J. Layfield, J. M. Bean, L. R. Prosnitz, and M. W. Dewhirst, Cancer Res. **56**, 941–943 (1996).

[263] P. Okunieff, M. Hoeckel, E. P. Dunphy, K. Schlenger, C. Knoop, and P. Vaupel, Int. J. Radiat. Oncol. Biol. Phys. **26**, 631–636 (1993).

[264] B. Chance, E. Anday, S. Nioka, S. Zhou, L. Hong, K. Worden, C. Li, T. Murray, Y. Ovetsky, D. Pidikiti, and R. Thomas, Opt. Express **2**, 411–423 (1998).

[265] M. A. Franceschini, V. Toronov, M. E. Filiaci, E. Gratton, and S. Fantini, Opt. Express **6**, 49–57 (2000).

[266] B. Chance, Z. Zhuang, UnAh Chu, C. Alter, and L. Lipton, Proc. Natl. Acad. Sci. USA **90**, 2660–2774 (1993).

[267] Y. Hoshi, Y. Onoe, Y. Watanabe, J. Andersson, M. Bergstrom, A. Lilja, B. Langstom, and M. Tamura, Neurosci. Lett. **172**, 129–133 (1994).

[268] S. P. Gopinath, C. S. Robertson, R. G. Grossman, and B. Chance, J. Neurosurg. **79**, 43–47 (1993).

[269] C. S. Robertson, S. P. Gopinath, and B. Chance, J. Biomed. Opt. **2**, 31–41 (1997).

[270] H. Ghalenoui, H. Saidi, M. Azar, S. T. Yahyavi, H. B. Ravazi, and M. Khalatbari, Prehosp. Disaster Med. **23**, 558–561 (2008).

[271] K. Svanberg, N. Bendsoe, J. Axelson, S. Andersson-Engels, and S. Svanberg, J. Biomed. Opt. **15**, 041502 (2010).

[272] M. S. Thompson, A. Johansson, T. Johansson, S. Andersson-Engels, S. Svanberg, N. Bendsoe, and K. Svanberg, Appl. Optics **44**, 4023–4031 (2005).

[273] J. Swartling, J. Axelsson, G. Ahlgren, K. M. Kälkner, S. Nilsson, S. Svanberg, K. Svanberg, and S. Andersson-Engels, J. Biomed. Opt. **15**, 058003 (2010).

[274] L. Lilge, N. Pomerleau-Dalcourt, A. Douplik, S. H Selman, R. W Keck, M. Szkudlarek, M. Pestka, and J. Jankun, Phys. Med. Biol. **49**, 3209–3225 (2004).

[275] R. Bays, G. Wagnières, D. Robert, D. Braichotte, J.-F. Savary, P. Monnier, and H. van den Bergh, Las. Surg. Med. **20**, 290–303 (1997).

[276] V. Ntziachristos, X. Ma, and B. Chance, Rev. Sci. Instrum. **69**, 4221–4233 (1998).

[277] L. Thrane, R. H. Jacobsen, P. Uhd Jepsen, and S. R. Keiding, Chem. Phys. Lett. **240**, 330–333 (1995).

[278] Y. Y. Wang, T. Notake, M. Tang, K. Nawata, H. Ito, and H. Minamide, Phys. Med. Biol. **56**, 4517–4527 (2011).

[279] T. Schlauch, M. Li, M. R. Hofmann, A. Klehr, G. Erbert, and G. Tränkle, Electron. Lett. **44**, 678–679 (2008).

[280] C. Jördens, T. Schlauch, M. Li, M. R. Hofmann, M. Bieler, and M. Koch, Appl. Phys. B **93**, 515–520 (2008).

[281] R. M. Woodward, V. P. Wallace, D. D. Arnone, E. H. Linfield, and M. Pepper, J. Biol. Phys. **29**, 257–261 (2003).

[282] V. P. Wallace, A. J. Fitzgerald, E. Pickwell, R. J. Pye, P. F. Taday, N. Flanagan, and T. Ha, Appl. Spectrosc. **60**, 1127–1133 (2006).

[283] A. J. Fitzgerald, V. P. Wallace, M. Jimenez-Linan, L. Bobrow, R. J. Pye, A. D. Purushotham, and D. D. Arnone, Radiol. **239**, 533–540 (2006).

[284] H. Chen, W.-J. Lee, H.-Y. Huang, C.-M. Chiu, Y.-F. Tsai, T.-F. Tseng, J.-T. Lu, W.-L. Lai, and C.-K. Sun, Opt. Express **19**, 19523–19531 (2011).

[285] P. C. Ashworth, E. Pickwell-MacPherson, E. Provenzano, S. E. Pinder, A. D. Purushotham, M. Pepper, and V. P. Wallace, Opt. Express **17**, 12444–12454 (2009).

[286] F. Wahaia, G. Valusis, L. M. Bernardo, A. Almeida, J. A. Moreira, P. C. Lopes, J. Macutkevic, I. Kasalynas, D. Seliuta, R. Adomavicius, R. Henrique, and M. Lopes, J. Mol. Struct. **1006**, 77–82 (2011).

[287] M. Uemukai, H. Ishida, A. Ito, T. Suhara, H. Kitajima, A. Watanabe, and H. Kan, Jpn. J. Appl. Phys. **51**, 020205 (2012).

[288] K. H. Park, N. Kim, H. Ko, H.-C. Ryu, J.-W. Park, S.-P. Han, and M. Y. Jeon, Proc. SPIE **8261**, 826103 (2012).

[289] N. Kim, S.-P. Han, H. Ko, Y. A. Leem, H.-C. Ryu, C. W. Lee, D. Lee, M. Y. Jeon, S. K. Noh, and K. H. Park, Opt. Express **19**, 15397–15403 (2011).

[290] A. Khorsandi, S. G. Sabouri, S. Fathi, and M. Asadnia-Jahromi, Opt. Laser Technol. **43**, 956–959 (2011).

[291] M. Chi, O. B. Jensen, and P. M. Petersen, Opt. Lett. **36**, 2626–2628 (2011).

[292] C. Brenner, M. Hofmann, M. Scheller, M. K. Shakfa, M. Koch, I. C. Mayorga, A. Klehr, G. Erbert, and G. Tränkle, Opt. Lett. **35**, 3859–3861 (2010).

[293] P. Bakopoulos, I. Karanasiou, N. Pleros, P. Zakynthinos, N. Uzunoglu, and H. Avramopoulos, Meas. Sci. Technol. **20**, 104001 (2009).

[294] D. Molter, A. Wagner, S. Weber, J. Jonuscheit, and R. Beigang, Opt. Express **19**, 5290–5296 (2011).